University of Alberta

Catalytic Combustion of Lean Methane on Commercial Palladium-Based Catalysts

by

Guangyu Huang

A thesis submitted to the Faculty of Graduate Studies and Research
in partial fulfillment of the requirements for the degree of

Master of Science

in

Chemical Engineering

Department of Chemical and Materials Engineering

Spring 2010

Edmonton, Alberta

Examining Committee

Robert E. Hayes, Chemical and Materials Engineering

Sieghard E. Wanke, Chemical and Materials Engineering

M. David Checkel, Mechanical Engineering

Life achieves its summit when it does to the utmost that which it was equipped to do

- Jack London, *White Fang*

Dedication

I would like to dedicate this work to my parents and my friends. Mom and Dad, I always feel lucky to be your child. My dear friends, as it said in the Bible, two are always better than one.

Abstract

Catalytic combustion provides us an efficient approach for the utilization and mitigation of methane, the major component of natural gas as well as an important greenhouse gas in global warming. From the research of catalytic combustion of methane, better understandings as well as solutions to the current methane-related problems can be obtained.

This study investigates lean methane combustion on palladium-based catalysts. Catalysts' activities were tested through ignition and extinction experiments. Several pretreatments and their influence were studied. Instrumental neutron activation analysis (INAA) and x-ray diffraction (XRD) were used as characterization tools for the catalysts. It was found that after being reduced, catalysts had stable and excellent abilities for methane conversion. However, these abilities were strongly compromised by additional water in the feeds. XRD results, combined with other testing results, implied that reduction produced the most active samples, while INAA revealed the real Pd concentrations of these catalysts.

Acknowledgement

First and foremost, I would like to give my sincerest appreciate to my supervisor, Dr. Robert E. Hayes, whose enthusiasm, wisdom, and patience provided me an wonderful opportunity to study and experience, advised me on this research project, taught me how to “tell a good story” with experimental results, and guided me with his words and actions in every way within these twenty-six months. Without his instruction, my graduate study cannot from blueprint become reality.

I am also entirely grateful of Dr. Sieghard E. Wanke. His astounding knowledge and insight gave me indispensible and priceless advisory, not only on this project, but also on general research and study of science and technology. His optimism always encouraged me, and his strictness towards every details made me know how to cut a rough diamond into a gem. Besides, I want to thank his help on this thesis.

I deeply appreciate Natural Science and Engineering Research of Canada which provides the funding for my graduate study and research from. Umicore AG of Germany also deserves special thanks for the generous supply of the catalysts used in my research.

I want to thank Dr. Long Wu, who untiringly helped me on the build of the reaction system, on the use of lab equipments, and even one the culture and situation in Canada which was new to me. I would also like to give my gratitude to Dr. Joseph Mmbaga, for his patient answer to my every question, and nice conversations from time to time. Finally, I want to thank the staff of Department of Chemical and Materials Engineering, University of Alberta. I feel warm at this place because of your help.

Table of Contents

1. Introduction ……...……..…... 1

1.1 Background ……...……...… 1

1.1.1 Greenhouse gas and methane emission mitigation 2

1.1.2 Risk control in coal mines ……..……..… 4

1.2 Catalytic combustion: A potential solution ……....…….. 5

1.3 Scope of work ……..…… 5

1.4 Structure of this thesis ……..……..... 6

2. Literature review ……...……..…….. 7

2.1 History and advantages of catalytic combustion …...…….. 7

2.2 Catalysts ……..……...…..…… 8

2.2.1 Rare earth materials and other oxides ……...……..….. 9

2.2.2 Noble metals ……..……..…..……. 11

2.3 General patterns of catalytic methane combustion on Pd catalysts…….16

2.3.1 Behavior of catalytic methane combustion ……...…..… 16

2.3.2 Mechanism of catalytic methane combustion on Pd…..... 18

3. Experiments and procedures ……..……. 20

3.1 Experimental apparatus & materials …….....….... 20

3.2 Experiment procedures ……..……..…... 24

3.2.1 Reactant Compositions ……..……..……... 24

3.2.2 Ignition and extinction curves of methane combustion ….. 24

3.2.3 Reduction and oxidation ……..…..……. 25

3.2.4 Catalysts' performance at high temperature ……...…..….... 26

3.3 Catalyst characterization ……..…….. 26

3.3.1 Instrumental Neutron Activation Analysis (INAA) …… 26

3.3.2 X-Ray Diffraction (XRD) ……...…….... 27

4. Results and analysis ……....…… 28

4.1 Preliminary tests ……..…….…….. 28

4.1.1 Tests without any pretreatments ……..…. 28

4.1.2 Tests with ageing pretreatments ……...…..…. 39

4.1.3 The effects of reduction pretreatments ……...……..... 45

4.2 Ignition and extinction curves ……..……...…… 49

4.2.1 Unusual trend of ignition and extinction curves ...…..…… 49

4.2.2 Methane concentration effects ……...……..…… 56

4.2.3 The effect of added water ……...……..….... 64

4.3 Methane combustion on different Pd states ……..…. 78

4.3.1 The performance of catalysts at high temperature ……. 78

4.3.2 The influence of reduction and oxidation ……...……... 78

4.4 Characterization of catalysts and analysis ……...…..….... 86

4.4.1 Instrumental Neutron Activation Analysis (INAA) …..… 86

4.4.2 X-Ray Diffraction (XRD) ……..…….. 87

5. Summary and Future Work ……..…..…… 95

5.2 Sumary……..…….……..……...95

5.1.1 General behaviours of the catalysts ……....……..… 95

5.1.2 Influence of various pretreatments ……..……..… 95

5.1.3 Influence of methane concentration ……....……..… 95

5.1.4 Influence of addition of water in the feeds……..… 96

5.1.5 Preliminary characterization……..……..… 96

5.2 Future work……..……..……...97

5.2.1 Gas constituents ……..……...……..…… 97

5. 2.2 Kinetics and temperature profile inside of the reactor …... 97

5. 2.3 Various pretreatments ……...…….. 98

5. 2.4 Catalyst characterizations ……..……...…… 98

5. 2.5 Pt-Pd bimetallic catalysts ……....….. 99

5. 2.6 Further study on catalyst deactivation and recovery ..…. 100

References ……...……...…… 101

Appendix A: Run list ……..…… 107

List of Tables

Table 4.1 List of runs for methane oxidation ……..… 30

Table 4.2 Instrumental Neutron Activation Analysis results ….. 87

List of Figures

2.1 Catalytic Combustion of Hydrocarbon as a function of temperature, adopted from Lee and Trimm (1995) ……..…….....…17

3.1 Sketch of the testing system ……...……..……..…...……21

3.2 Photo of the testing system ……...……..…….…..…..…22

3.3 Catalyst samples, 150, 80, 15 g/ft^3 (left to right) ……..…..……...…22

4.1 Ignition & extinction of methane combustion Run#: 0401, 0402..... 36

4.2 Ignition & extinction of methane combustion Run#: 0403, 0404….. 37

4.3 Ignition & extinction of methane combustion Run#: 0405, 0406 ….. 38

4.4 Ignition & extinction of methane combustion Run#: 0410, 0411 ….. 40

4.5 Ignition & extinction of methane combustion Run#: 0412, 0413 ….. 41

4.6 Ignition & extinction of methane combustion Run#: 0414, 0415 ….. 42

4.7 Ignition & extinction of methane combustion Run#: 0400, 0421 ….. 43

4.8 Ignition & extinction of methane combustion Run#: 0422, 0423 ….. 44

4.9 Ignition & extinction of methane combustion Run#: 0426, 0427 ….. 46

4.10 Ignition & extinction of methane combustion Run#: 0428, 0429..... 47

4.11 Ignition & extinction of methane combustion Run#: 0430, 0431..... 48

4.12 Ignition & extinction curves of methane combustion, reduced Run#:0701,0702 ……...….... 51

4.13 Ignition & extinction curves of methane combustion, reduced

Run#: 0506, 0507 ……..……...…..... 52

4.14 Ignition & extinction curves of methane combustion, reduced

Run#:0601,0602 ……...……..... 53

4.15 Comparison of ignition of Pd loadings; Run#: 0505, 0601, 0701..... 54

4.16 Comparison of extinction of Pd loadings; Run#:0505,0601,0701 55

4.17 Ignition and extinction curves of methane combustion: methane

effects; Run#:0610, 611 ……..……..……..... 58

4.18 Ignition and extinction curves of methane combustion: methane

effects; Run#:0605, 0606 ……..…….…..….....…..... 59

4.19 Ignition and extinction curves of methane combustion: methane

effects; Run#:0608, 0609 ……..……...……...…..... 60

4.20Comparison of ignition curves with different methane concentrations

Run#:0605, 0608, 0610 …….....……...…..... 61

4.21 Comparison of extinction curves with different methane

concentrations; Run#:0606, 0609, 0611 ……...…...……..…..... 62

4.22 Amount of converted methane at ignition with different methane

concentrations; Run#: 0605, 0608, 0610 …….…..... 63

4.23 Ignition and extinction curves of methane combustion: water effects

Run#: 0901, 0902 ……..…….....……...…..... 66

4.24 Ignition and extinction curves of methane combustion: water effects

Run#: 0903, 0904 ……..……...……...…..... 67

4.25 Ignition and extinction curves of methane combustion: water effects

Run#: 0905, 0906 ……..……...…….....…..... 68

4.26 Ignition and extinction curves of methane combustion: water effects

Run#: 0907, 0908 ……..……...……...….... 69

4.27 Ignition and extinction curves of methane combustion: water effects

Run#: 0913, 0914 ……..……...……...…..... 70

4.28 Ignition and extinction curves of methane combustion: water effects

Run#: 0915, 0916 ……..…….....……...….... 71

4.29 Deactivation Test with additional water, Run#: 0919 ……...….... 72

4.30 Ignition and extinction curves of methane combustion: water effects;

Run#: 0923, 0924 ……..……...……...….... 73

4.31 Ignition and extinction curves of methane combustion: water effects;

Run#: 0925, 0926 …….……..……..…….... 74

4.32 Ignition and extinction curves of methane combustion: water effects;

Run#: 0927, 0928 ……....….... 75

4.33 Ignition and extinction curves of methane combustion: water effects

Run#: 0929, 0930 ……...……..…….... 76

4.34 Deactivation test with extra water then cutting off, Run#: 0932..... 77

4.35 The high temperature extinction curve for methane combustion

Run#: 0430 ……..……...…….....…..... 81

4.36 Comparison among extinction branches of different states

Run#: 0702, 0703, 0704 ……...……..... 82

4.37 Comparison among extinction branches of different states

Run#: 0502, 0509, 0510 ……...……...….... 83

4.38 Comparison among extinction branches of different states

Run#: 0606, 0607, 0613 ……...……...……..... 84

4.39 Comparison among extinction branches with varied oxidizing times

Run#: 0613, 0616, 0617 ……...…….…..... 85

4.40 XRD patterns for untreated, reduced and oxidized samples ….….. 90

4.41 XRD patterns for concentrated Pd samples: Untreated, reduced and oxidized ….……...…….……..…..... 91

4.42. Expanded XRD patterns for plots shown in Figure 4.41 of concentrated Pd samples: Reduced and oxidized ……...….... 92

4.43. Difference XRD pattern obtained by subtraction of the oxidized pattern in 4.42 form the reduced pattern in 4.42 ..……..….... 93

4.44. Effect of increased counting time per step on XRD patterns for reduced concentrated sample ……..……..….... 94

Symbol	Description	Unit
d_{avg}	the average crystal diameter	nm
λ	the wave length of the CuKα radiation	nm
FWHH	the width at half height of the diffracted peak	°2θ
θ	half of the diffraction angle	°

List of acronyms

CFRR	Catalytic Flow Reversal Reactor
FCC	Face-centered cubic
FWHH	Full widths at half height
GC	Gas chromatograph
GHG	Greenhouse Gas
GWP	Global warming potential
I-E	Ignition and extinction
INAA	Instrumental neutron activation analysis
IPCC	Intergovernmental Panel on Climate Change
LSA	Low surface area
ppm	Parts per million
SS	Stainless steel
TC	Thermocouple
TEM	Transmission electron microscopy
TGA	Thermogravimetric Analysis
UHP	Ultrahigh purity
USA	United States of America
VOC	Volatile organic compound
XPS	X-ray photoelectron spectroscopy
XRD	X-ray diffraction

Chapter 1 Introduction

1.1 Background

Fossil fuels play a dominant role in our era. On one hand, they are the major energy source, which support our society like Atlas supporting the world. On the other, they also produce a large amount of pollution. Partial solutions related to the growing global demand of energy and the associated environmental problems include: innovation of alternate energy sources, such as biodiesels and solar energy, and improvements in current fossil fuel technologies making them more efficient and cleaner. Combustion of natural gas, consisting primarily of methane, is the cleanest and most efficient of all the fossil fuels due to lower production of sulphur dioxide and the oxides of nitrogen (NO_x) and more release of thermal energy per unit of carbon dioxide produced. Hence it has been widely applied in power generation (peaking power plants), automobile fuels (natural gas engines) and so on.

The complete combustion of methane can be represented with the following overall reaction:

$$CH_4 + 2O_2 \rightarrow CO_2 + 2H_2O \qquad (1.1)$$

However, conventional burning of natural gas still suffers from several shortcomings. Theoretically, the only products from methane combustion are water and carbon dioxide, but in conventional combustion, natural gas is usually burnt at about 2000 K. At this temperature, oxides of nitrogen will be generated, especially NO and NO_2, two toxic gases which are precursors for acid rain. Also, in many combustion applications, conversion of methane is

not complete, and thus the effluent usually contains some methane.

The homogenous combustion of methane can only occur in a certain range of fuel to air ratios, i.e. within the flammability limits. For methane the flammability limit ranges from 5 to 16 % by volume methane in air. This means lean methane mixtures are hard to combust, and thus not suitable as a fuel in conventional combustion.

These shortcomings lead to constraints on the application of natural gas combustion. For instance, special materials are needed for the reactors to stand the high burning temperature; the reaction must be initiated by a spark for ignition; both natural gas and air flow rates should be well controlled to make them mix under the flammability limits. Finally, the exhausted gases from the outlet of the reactor have to undergo further treatment to eliminate the oxides of nitrogen for environmental protection.

1.1.1 Greenhouse gas and methane emission mitigation

Global warming is one of the most serious issues we are facing today. According to Intergovernmental Panel on Climate Change (IPCC), the global warming since the middle of last century is largely caused by the excessive release of greenhouse gas (GHG) from human being's activity, such as combustion of fossil fuel, which might lead to global air temperature increases of 1.1 to 6.4°C during the twenty-first century, in contrast to 0.74 ± 0.18°C increase during the twentieth century; these temperature changes will probably bring about severe outcomes including rises of sea levels and change in precipitation patterns. ("Summary for Policymakers" by IPCC: *Climate Change 2007: The Physical Science Basis. Contribution of Working Group I to the Fourth Assessment Report of the Intergovernmental Panel on Climate Change*. http://ipcc-wg1.ucar.edu/wg1/Report/AR4WG1_Print_SPM.pdf, July

25th, 2009). Notice that in recent years a cooling trend of global temperature has been observed since 1998, the hottest year on human record.

In the discussions about GHG, carbon dioxide (CO_2) is usually given the most consideration, but methane is also a potent GHG.. Carbon dioxide makes up 9-26 % of all GHG, while methane, the second most important GHG, contributes 4 – 9 % to the GHG (Kiehl, J. T.; Kevin E. Trenberth, February 1997. "Earth's Annual Global Mean Energy Budget". *Bulletin of the American Meteorological Society* **78** (2): 197–208.). If water, the prime greenhouse gas, is excluded, CO_2 will be the top on the GHG list, up to 65%, and methane is the second. Although the worldwide molar release of methane is much less than the moles of CO_2 released, the potency of methane per kg is 23 times that of a kg of CO_2 on global warming potential (GWP). Equation 1.1 shows that during methane combustion one mole methane is converted into one mole carbon dioxide. CO_2 has a much lower greenhouse effect per mole than methane. Burning 16 tonnes of methane gives 44 tonnes of CO_2, but the methane has 23 times the GWP, thus it will result in an 88 % reduction of overall GWP. Therefore, the conversion of fugitive emissions of methane to carbon dioxide emissions results in a large decrease in GHG.. Homogenous combustion of methane requires relatively high concentrations of methane in air, and exhaust gases from many oil, gas and petrochemical processes, and gases vented from coal mines, have low concentrations of methane that are frequently vented into the atmosphere.

A large portion of methane emission comes from oil and gas industries. In 2006, about 343 million metric tons carbon dioxide equivalent of methane were emitted by the oil and gas sector, 18% of total global emissions. Specifically, in Canada, 50 % of the GHG from the oil and gas sector is in the form of fugitive methane emissions. Mainly, these emissions in oil and gas industries come from extraction, processing, storage and distribution in terms

of leakage, venting or incomplete burning. As stated in *Canada's 2007 Greenhouse Gas Inventory*, 747,000 (kt CO_2 eq) greenhouse gases were emitted in Canada in 2007, of which 64,800 from fugitives, including 21,300 from natural gas, 31,700 from venting, i.e. fugitive emissions contributed less than 10 % of total emissions in Canada., Although this is not a very high percentage, a significant reduction in the fugitive emissions would go a long way towards meeting Canada's commitment to the Kyoto Protocol of a reducing GHG emissions to a level which is 6 % below the 1990 level for the 2008 to 2012 period.

1.1.2 Risk control in coal mines

Risk control in coal mines was the very motivation for Sir Humphrey Davy to conduct his research on methane combustion in the early 19th century; in these studies he discovered catalytic combustion. Methane, often present in coal, can accumulate in mines to the explosive range and become ignited by a spark; such methane explosions are frequently the cause of fatal explosions in underground coal mines. Sadly, after nearly two hundred years, methane remains a serious problem in many coal mines, especially in developing countries, such as China and India, causing hundreds of miners' deaths annually. Just two years ago, in 2007, a methane explosion located more than one kilometre below the ground level took 101 lives at Zasyadko coal mine in the Ukraine.

Although gas explosions in mines are less frequent in more developed countries of North America and Europe, they still occur. In 1992, a gas explosion took the lives of 26 miners at Westray Mine in Nova Scotia, Canada, and more recently, in 2006, 12 miners were killed by a gas explosion at the Sago Mine in West Virginia, USA. One of the effective approaches to solve the latent danger of methane is the catalytic flow reversal reactor, an efficient

equipment to combust lean methane mixtures that will be introduced later in this chapter.

1.2 Catalytic Combustion: A Potential Solution

Catalytic combustion was discovered by Sir Humphrey Davy in the early nineteenth century. It has several unique features that distinguish itself from traditional homogeneous combustion (Hayes and Kolaczkowski, 1997). For instance, there is no flame in catalytic combustion, due to which it is also called flameless combustion. What is more, catalytic combustion usually proceeds at lower temperature, leading to less generation of nitrogen oxides, and less constraints on reactor design. More advantages of catalytic combustion will be introduced later in the second chapter.

Thanks to these amazing merits, catalytic combustion has prospered for the last thirty years from laboratories to factories. Nowadays this technique, especially its branch in methane combustion, still draws lots of attention. It is a desirable alternative for homogeneous combustion in many industrial applications, such as catalytic converters of volatile organic compounds and natural gas engines because the process of catalytic combustion is cleaner and less expensive than alternate methane removal techniques. In petrochemical plants, it can considerably reduce the generation of some contaminants which are inevitable in homogeneous combustion, while in coal mines, it can be used to mitigate the fugitive gases and hence avoid explosions. In a word, catalytic combustion is a potential solution for many problems caused by methane.

1.3 Scope of work

The purpose of this project is to explore the effects of using commercial palladium-based monolith catalysts for the combustion of lean methane mixtures, by the following tests:

1. The catalytic reaction of methane combustion was tested under various experimental parameters, including different temperatures, different feeds compositions, and different Pd loadings;

2. Several pretreatment methods with their impacts were studied.

Based on the results, the behaviour of catalysts will be quantified for the development of catalytic flow reversal reactor (CFRR, Salmons et al., 2003). In addition, the experiments are also done for the appealing application of these catalysts in natural gas internal combustion engines for exhaust gas after treatment, so extra water feeds was added to simulate the compositions of exhausted gases from natural gas engines.

1.4 Structure of this thesis

There are five chapters in this thesis. Chapter 1 shows the situations and problems of methane emissions, and the technique of catalytic combustion as a solution is introduced with the major motivations for this project. Former studies and literatures in this area are then reviewed and summarized in Chapter 2. Chapter 3 describes the apparatus, procedures and materials involved in experiments as well as catalyst characterizations, while their results are analyzed in Chapter 4. Summary of current research with potential work on this topic that is worthwhile for future investigation is listed in the final part, Chapter 5.

Chapter 2 Literature Review

2.1 History and Advantages of Catalytic Combustion

The phenomenon of catalytic combustion of methane has emerged in our vision since 1818, when Sir Humphrey Davy, who was asked to study safety-lamps in coal mines, discovered that oxygen and methane (main components of gases in coal mines) in contact with hot platinum wires would produce a considerable amount of heat without generating flames. From then on, with the prosperity and bloom in general catalysis, more and more research was carried out in the area of catalytic combustion. In the 1960s, catalytic convertors became an appealing topic of research, and in 1970s William C. Pfefferle invented the first catalytic combustor to reduce the formation of nitrogen oxides and carbon monoxides from gas turbine engines.

Recently catalytic combustion of methane has drawn considerable attention based on its various applications, especially in energy and transportation industries with environmental concerns. With the foreseeable depletion of crude oil, natural gas will become one of the main sources of energy. On one hand, compared with other fossil fuels, natural gas contains less nitrogen and sulphur, and yields lower amount of CO_2 per energy unit during combustion. On the other hand, methane has a greenhouse effect twenty-three times larger than CO_2, which means there will be significant GHG emissions from production, storage and distribution of natural gas.

Compared with homogenous combustion, catalytic combustion (flameless combustion) of methane has two main advantages:

1. Catalytic combustion can occurs at temperatures much lower than homogenous combustion. This means less heat lost, more available materials for the combustion reactors, easier to control the reaction, and most importantly, less nitrogen oxides (NO_x) generation;

2. Catalytic combustion has no flammability limit. This is a necessary range of compositions, or certain ratios of fuel to air within which homogenous combustion can happen. For instance, methane can combust in air only when it has a proportion of 5 % to 16 % by volume in air. Higher or lower than these limits, there is no homogenous combustion.

Due to these advantages, catalytic combustion has been widely applied in many areas, from small catalytic hair curlers, to catalytic converters of volatile organic compounds (VOCs). Catalytic combustion can provide us exceptional solutions to the methane problems such as fugitive emissions and potential dangers of methane in coal mines discussed above.

2.2 Catalysts

Both supported and non-supported catalysts has been studied for catalytic methane combustion. In supported catalysts, the catalysts are dispersed on another material, so the surface area of catalytic materials is increased, and supports and catalysts often interact with each other. As a result, supported catalysts usually have better performance because catalyst particles are well dispersed on the supports which have a large surface area and high surface to volume ratio, resulting in more active sites. Secondly, catalysts will be more stable with the help of supports. As the core of catalytic combustion system, an ideal catalyst and its supports will have certain qualities:

1. High activity;

2. Low ignition temperature: as said above, a low combustion temperature will reduce the generation of NO_x, and pose less severe limits on reactor design;

3. High thermal stability: methane combustion is a extremely exothermic reaction, and the temperature of the catalytic system will quickly increase once the reaction is started. With the existence of heat transfer limit, temperature on the catalysts is usually higher than that of gas phase. So thermal stability is crucial to the overall properties of the catalysts

4. Stable activity and high resistance to poisons;

5. Low price;

6. Nontoxic.

Unfortunately, no catalyst can perfectly fulfill all the above requirements, but they are still desirable standards by which different catalysts can be judged.

2.2.1 Rare earth materials and other oxides

Rare earth materials and metal oxides can be directly used as catalysts without further modification. Choudhary and Rane (1992) tested the catalytic activity for methane conversion of several rare earth oxides using a pulse microreactor, and found that at 1073 K, with presence of oxygen, the activities of these oxides were: $Sm_2O_3 > La_2O_3 > Yb_2O_3 > Eu_2O_3 > CeO_2$, none of which was satisfying considering the fact that less than 30% of methane was converted on these catalysts. Other single oxides of transition metals like CuO, Mn_3O_4 also have some activity.

Rare earth metals can also be used as addictives to promote the catalytic activity of other metal oxides. Choudhary et al., (1997) studied the methane conversion and surface properties on rare earth doped MgO catalysts with different rare earth over manganese ratio at 650-850°C, and found that the

presence of all rare earth promoters increased the activity of MgO catalysts appreciably, particularly Ce-MgO and Eu-MgO, because rare earth doping resulted in a large increase on the basic sites of the catalysts and a decrease on the acid sites. This kind of catalysts can be presented by the general formula of A-BO_x, where A is the rare earth metal promoter, and BO_x is the metal oxide. Other doped catalysts of metal oxides are also popular, e.g. alkali metal doped oxides, metal chloride promoted oxides and transition metal (Cr, Fe) doped ZrO_2 or SnO_2. Notice that for some doped catalysts with metal chloride, the promoters are inclined to evaporate at the high temperature during the reaction, causing the quick and unrecovered deactivation of the catalysts.

Perovskite-type catalysts are another choice. Perovskite-type oxides are mixed metal oxides with a face-centered cubic (FCC) structure and a general formula ABO_3 which have been used in many area, such as the research of superconductivity materials, transistors and fuel cells. For perovskite-type catalysts ABO_3 in catalytic methane combustion, metals in site A is often rare earth or lanthanide elements, and metals in site B is a transition metal. Sometimes metals in the A site provide the structural stability, metals in the B site are responsible for the catalytic activity, $LaFeO_3$ is an example of this case. At other times metals in A and B can work together to form an outstanding catalyst, like $PbMgO_3$. The most popular A metal is La, and the most popular B metals are Mn or Co.

The base metal catalysts have both advantages and non-negligible drawbacks. The main advantage is that they are relatively inexpensive compared with noble metals.. The main disadvantage is their low activity and high temperatures (usually more than 1000 K) are required to achieve good conversion. As a result, base metal catalysts are not as popular as noble metals in both academic research and industrial applications.

2.2.2 Noble metals

Among all noble metal catalysts, platinum and palladium are the most appealing because they have excellent activity at low temperature and are very stable, although not very abundant in supply. Various efforts have been made on the comparison of these two catalysts, and their performance is distinguished in many ways.

At lower temperature (below 1100 K), palladium, in the presence of oxygen, will be oxidized, into PdO. For platinum, PtO_2 can hardly be generated below 825 K and is very unstable. Since PdO is much more stable than PtO_2, at this range the active phase is metallic Pt for platinum and PdO for palladium. PdO is usually more active than Pt, and thus palladium catalysts often show higher activity than platinum catalysts, especially on methane lean side. Influenced by various of conditions such as Pd loadings, supports and pretreatments, a range of results have been reported by researchers on the specific activity of Pd catalysts. For instance, Machocki et al., (2009) examined the catalytic activities of Pd/Al_2O_3 and Pt/Al_2O_3 both with metal loadings of 0.41 % (wt), and found that the reaction on Pd catalysts was activated at 400°C. The light-off temperature is 500°C and methane is completely converted at 700°C. Salaun et al., (2009) investigated the abilities of 2.55 % (wt) Pd/silica to degrade a gas mixture of NO, CH_4, CO and traces of CO_2 and H_2. It was shown that the reaction started at 250°C, ignited at 325°C and reached 100% conversion at around 400°C, almost independent of methane concentrations. For Pt catalysts, these three temperatures were 450°C, 675°C and 900°C, respectively. However, platinum catalysts have better resistance to poisons such as sulphur species (Meeyoo et al., 1998) and water (Gelin et al., 2003), and platinum particles are less likely to sinter at relatively low temperatures (Hurtado et al., 2004), so their general performance is more stable and enduring than palladium catalysts. Last of all, platinum is relatively “simple”,

whilst the phase transformation of palladium is very complex, and most of the related topics, such as whether Pd or PdO is more active, remain highly controversial. In this thesis the research was done on palladium-based catalysts, so from now on major attention will be on Pd catalysts.

a. Supported Pd catalysts

Supports and dopings: As stated above, supported catalysts have many advantages over non-supported catalysts, and are the mainstream of research on catalytic methane oxidation. The dispersion of Pd particles on supports results in higher Pd areas per unit Pd as well as improvements in the thermal stability compared to bulk metal catalysts. Meanwhile, some supporting materials can interact with the reactants leading to a stronger resistance to poisons and even higher activity. Some supports can prevent the supported metal particles from sintering, which results in longer life for the catalytic system. Consequently, the research on catalysts supports is as important as on the catalytic material itself. The most commonly used supports for catalytic methane combustion are transition alumina (γ-Al_2O_3 being the most common), silica, zirconia, titania and molecular sieves (complex metal oxides or active carbon). γ-aluminas used to be by far the most popular supports, given that they have large surface areas, are inexpensive and have the ability to inhibit the mobility of Pd species which results in good thermal stability, i.e. reduces the rate of Pd sintering. However, at high temperature (around 1275 K), the γ-phase of alumina becomes unstable and transform to the α-phase; this phase change is accompanied by a drastic lost of surface area and a large reduction in the concentration of accessible active sites. This was also observed on some other supported Pd catalysts such as CeO_2, ZrO_2 and silica by Gelin et al., (2002) and Escandon et al., (2005), who observed that catalytic activities of these catalysts decreased with time, due to the sintering of Pd particles or the supports. (Sintering of Pd particles occurs by growth of the particles resulting in a decrease in Pd area; support sintering occurs by pore collapse or phase

changes resulting in encapsulation of the active Pd particles). It is not hard to imagine that most of the benefits of supported catalysts will be compromised by these phenomena. Several solutions have been posed to avoid sintering. The first is the use of mixed metal oxides. Ozawa et al., (2003) reported that the addition of Nd_2O_3 and La_2O_3 into Al_2O_3 effectively stopped the decrease of active sites and slow down the transformation from PdO to Pd. Secondly, supports can become more thermally stable with the modification of additional metal promoters.

Pretreatment and particle sizes: Pretreatment, by reduction in hydrogen or oxidation in oxygen, is another key parameter which affects the performance of supported Pd catalysts. In the work of Schmal et al., (2006) done on Pd/Al_2O_3 catalysts, same catalyst samples acted significantly different with or without reduction pretreatment. On reduced samples the light-off temperature decreased by almost 40°C and complete conversion was reached at 450°C, in contrast to 500°C on regular samples. Cullis et al., (1983) studied the influence of pretreatment procedures of Pd/Al_2O_3 with three gas sources: $He+H_2$, O_2 and H_2. He discovered that the activities of catalysts pretreated by $He+H_2$ were much higher than those pretreated in pure hydrogen or oxygen. This finding is in agreement with the results of Baldwin et al., (1990). Generally, reducing pretreatments with hydrogen will yield catalysts with higher activities for methane oxidation than oxidizing pretreatments in oxygen. Another influence caused by pretreatment procedures is the Pd particle size, partially discussed in the above section of "Supports and dopings". This effect can be represented by structure sensitivity considering the dependence of particle sizes and dispersions on the structures of catalytic systems. Roth et al., (2006) prepared and investigated catalytic abilities of $Pd/\gamma\text{-}Al_2O_3$ catalysts with various Pd sizes (ca. 2-30 nm in diameter) and different pretreatments. It was discovered that at 260°C, particles with sizes less than 12 nm had constant catalytic activities, whereas for those with sizes larger than 12 nm,

their activities decreased with the increasing of particle sizes. In addition, oxidation behaviours of catalysts are also vital as PdO and Pd have different contributions to methane oxidation. In the same work it was observed that smaller particles were oxidized faster, and the generated PdO was more stable than those produced on larger particles, leading to different catalytic performance among catalysts with different particles sizes. On the other hand, controversy remains on this issue when some researchers showed the results that particles size have no or trivial effects on catalytic activities. Cullis et al., (1983) investigated the sintering of particles on 2.7 wt.% Pd/γ-Al_2O_3 by a heat treatment for 40 days in oxygen at 550°C. When a large scale sintering was observed with SEM, there was no change on methane conversion. The same observation was made by Hoyos et al., (1993) on 2.2 wt.% Pd/SiO_2 catalysts. In spite of a 50% drop of metallic dispersion (measured with hydrogen chemisorption) by sintering, the light-off temperature only slightly decreased by 5°C.

Reaction conditions: Probably the most complicated parameters on the activity of supported Pd catalysts are reaction conditions, including feed composition, reaction temperature and pressure. The feed composition, with special emphasis on the methane to oxygen ratio, is of prime importance. Although flammability limits do not affect catalytic combustion, methane to oxygen ratio is still decisive because under oxygen rich conditions (lean methane), methane will be oxidized to CO_2, while on the oxygen poor side (rich methane), CO will be generated and methane conversion will be most likely be lower. Ideally, the feed for catalytic methane combustion has only methane and oxygen, but in reality even highly pure natural gas contains a slight amount of sulphur, which will poison catalysts, as discussed below. On the other hand, methane will come with CO, CO_2 and water as exhausted gases from petrochemical processes and natural gas engines. They are all harmful due to their inhibition of various steps in catalytic methane oxidation.

Last of all, for catalytic methane combustion on the methane lean side, it is widely accepted that methane concentration have no influence on the reaction (Ribeiro et al., 1994; van Giezen et al., 1999; Ciuparu et al., 2001).

Poisons: Poisons are the major cause of catalyst deactivation. Sulphur compounds are the most common and most severe poison for supported Pd catalysts. As observed by Arosio et al., (2005), Pd/Al_2O_3 catalysts lost nearly 90% of their activities with the presence of only 100 ppm H_2S, and the ignition temperature also raised by as much as 150 K, as the sulphur species was irreversibly absorbed by the catalysts. Chlorine is another important poison for supported Pd catalysts, but it has a different poisoning mechanism than sulphur. Another significant poison is water vapour, or moisture, which can be found within all kinds of methane exhausts. Lots of work has been made on this topic (Cullis et al., 1972; Ribeiro et al., 1994; van Giezen et al., 1999; Ciuparu et al., 2001). Water, especially additional vapour from feeds, will cause a huge inhibition to the reaction that is only partially reversible (Cullis et al., 1972). This is verified by Persson et al., (2007), who tested catalytic stability with water vapour on $Pd/\gamma\text{-}Al_2O_3$ (5% wt) prepared by incipient wetness impregnation. The temperature was fixed at 500°C, and water concentration studied were 1.25, 2.5, 5 and 10% by volume. It was shown that when no extra water is involved, the conversion of methane slightly dropped from 100% to 88% over an hour, while the decrease was much more severe when 5% additional water vapour was started: the conversion fell from 88% to 40% within only 20 minutes. Only part of the lost activity came back when extra water was stopped. In the measurement of van Giezen et al., (1999) on Pd/Al_2O_3 (7.3% wt), the apparent activation energy of catalytic methane combustion at dry state (no extra water feeds) was 86 kJ/mol between 200-320 °C, while this energy elevated to 151±15 kJ/mol with the presence of 2 vol. % extra water feeds. The effects of additional water are also influenced by other factors. Ciuparu et al., (2002) discovered that the lost

of activity caused by extra water could be completely recovered within an hour by simply cutting off the water feeds if the usually used HSA γ-Al_2O_3 was replaced by LSA α-Al_2O_3, and indicated that supports with high oxygen mobility might all have the same potential to mitigate the influence of water. Similar results were also achieved by adding certain addictives to Pd catalysts such as Pt (Persson et al., 2007) or rare earth materials (Cullis et al., 1972).

Temperatures: Reaction temperature affects the activity of supported Pd catalysts in two ways. Firstly, the apparent activation energy of methane combustion will change sharply with the elevation of temperature, and the rate of diffusion will also increase. Secondly, since the transformation between Pd and PdO will take place, the activity of Pd catalysts will change with an increase in temperature. Specifically, the activity of catalysts keeps increasing with temperature until around 975K, then the activity begins to fall with the continuously increase of temperature, since at this stage PdO thermally decomposing to Pd. This decrease will last until PdO is totally replaced by Pd at around 1050K. After that the activity will once again increase with temperature (Datye et al., 2000).

2.3 General Patterns of Catalytic Methane Combustion on Pd

2.3.1 Behavior of catalytic methane combustion

The general performance of supported Pd catalysts on catalytic methane combustion as a function of temperature is plotted in Fig. 2.1, adopted from the figure of Lee and Trimm (1995). Based on this, a typical catalytic methane combustion can be divided into three stages:

1. Low conversion stage, A-B: at low temperature the activity of catalysts is not high, and only low conversions are attained. Intrinsic surface reaction is the rate-limit step at this stage;

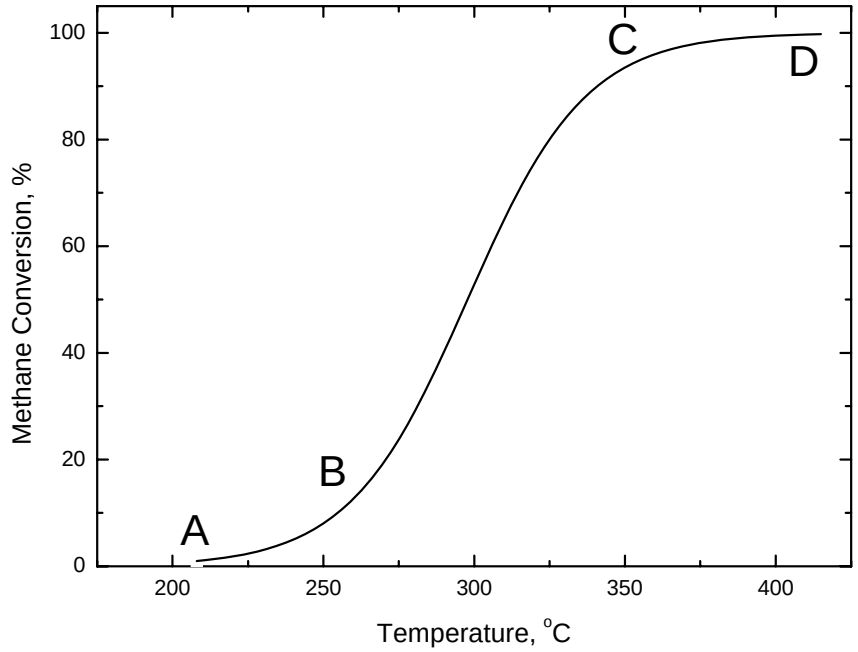

Figure 2.1 Catalytic Combustion of Hydrocarbon as a function of temperature, adopted from Lee and Trimm (1995)

2. Ignition (light-off) stage, B-C: when temperature increases to a certain level, catalysts are activated and the rate of diffusion are also much higher (Litto 2008) than stage A-B, so the reaction conversion increased rapid. Since methane combustion is highly exothermic, with the increase of conversion a large amount of heat is released, causing the further raise of temperature.

3. High conversion stage, C-D: at this stage the reaction stably continues. Mass and heat transfer become more important to the overall conversion, and at high temperature (above 1200 K) some methane is converted by the gas phase homogeneous reaction, not on the catalysts.

Most catalyst have the same S-shape curve, but the temperatures at which light-off occurs and the slopes of the S-shaped curves in the A-B-C regions depends very much on the type of catalyst and the feed composition.

2.3.2 Mechanism of catalytic methane combustion on Pd catalysts

Equation 1.1 shows the overall reaction for the complete combustion of methane, but it gives no indication of the complex surface reaction which occurs during the catalytic oxidation of methane. In contrast to platinum, which has a relatively uncomplicated surface structure and on which the catalytic methane combustion can be explained by simple reaction mechanism, the combustion on palladium is still controversial, on whether Pd or PdO is the active site, as well as on which mechanism should be applied. Most of researchers agree that the full combustion of methane is dominated by redox mechanisms, but they argue on which redox mechanism should be employed: Mars-van Krevelen type, or Langmuir-Hinshelwood type, or even other kinds such as Eley-Rideal.

Mars-van Krevelen mechanism declares methane is combusted with a

reduction-oxidation cycle of the catalysts. Methane first reacts with lattice oxygen from PdO on catalysts surface, resulting in the reduction of catalysts. Then the empty sites in the lattice are occupied by oxygen from gas phase, causing the re-oxidation of catalysts. Muller et al., (1996) proved this mechanism by investigating methane combustion over Pd/ZrO_2 catalysts with labelled $Pd^{18}O$, $H_2{}^{18}O$, $C^{18}O^{16}O$, and $^{16}O_2$, through which he discovered that at 300°C at least 20 % of the total produced CO_2 was related to lattice oxygen. The Mars-van Krevelen mechanism also gives an explanation for the fact that Pd is more active than Pt on methane lean side. According to the results from Niwa et al., (1983), Pt is harder to reduce, with a reduction temperature 120 ~ 200°C higher than Pd. This indicates that the reduction-oxidation cycle will be easier Pd catalysts, making them better at capturing smaller amount of methane than Pt. Fujimoto et al., (1998) proposed a detailed reaction procedure under Mars-van Krevelen mechanism with the theory that methane is first absorbed on the unsaturated Pd sites on the surface of PdO phase, and then hydroxyl Pd-OH species is formed via the transfer of a hydrogen atom from methane to PdO. The transfer of H is considered as the rate-limit step in this theory. Then CO_2 and H_2O will be generated through other detailed steps. It is worthwhile to recognize that the coexistence of Pd, PdO and Pd-OH here is very unstable, and fluctuation may take place at some temperatures. This could be an interesting justification for the puzzling phenomenon that sometimes temperature on the catalytic system and reaction rate both fluctuate with time, observed by Ozkan et al., (1997).

The Langmuir-Hinshelwood mechanism states that both methane and oxygen is absorbed on the catalysts, and they have to be close enough to start the reaction. In this mechanism lattice oxygen is not involved. The adsorption of reactants and desorption of products are not rate-limit steps.

Chapter 3 Experiments and Procedures

As discussed in Chapter 2, supported palladium catalysts are quite promising to solve many methane problems. Despite their wide acceptance in industrial applications, there are lots of controversies regarding to the general combustion behavior and catalytic mechanisms of Pd catalysts. Thus it is essential to design and conduct experiments on selected Pd catalysts to clarify these contentious issues.

Research in this project mainly focuses on four topics: 1. the general performance of commercial monolith Pd catalysts for natural gas automotives; 2. the effects of feeds composition such as methane and water vapour on the activities of catalysts; 3. the influence of pretreatments on catalytic activities; and 4. characterizations of catalysts as an explanation to experimental results.

Experimental equipment, materials, procedures and characterization settings are described in this chapter, and detailed results with discussions are given in the next chapter.

3.1 Experimental apparatus & materials

A reaction system was designed and used for all of the experiments in this project. The system included a micro-reactor, an oven, several gas and water supplies, and analyzers. Fig. 3.1 presents a diagram of the testing system, while Fig. 3.2 is a photograph of it.

Micro-reactor: The micro-reactor consisted of a 316 stainless steel (SS) tube (⅜″ dia. × 20″ long) concentrically connected at both ends with ¼″ diameter tubes. The latter are connected concentrically to ⅛″ diameter thermocouples, placed inside of a tube furnace An Opto 22 system was connected to the

system so that all the experiment conditions were automatically recorded on a computer by a software named Labview, although these parameters were set manually and controlled by a temperature controller and gas flow meters.

Catalysts: The catalysts in these experiments, provided by Umicore Group, were commercial palladium monolith catalysts designed to degrade the exhausted gases from natural gas combustion engines. Three Pd loadings were used, namely 150, 80 and 15 g/ft^3. According to this information, and assuming that washcoats account for 10 % of the total volume (based on the standards of many commercial automotive catalysts), it can be estimated that the Pd concentration of the three samples were 4.8, 2.6 and 0.48 wt %, respectively. To fit into the reactor, the monolith cores were crushed, ground and screened to particles with final sizes of 425 ~ 500 μm. A photo of the crushed catalysts is shown in Fig. 3.3.

Sensors and Analyzer: Temperature in these experiments was detected by three thermocouples (TC, K type from Omega). TC1 and TC2 were put into the reactor (tube), at the upstream (before the catalyst samples) and the downstream (after the catalyst samples), respectively. The temperature that

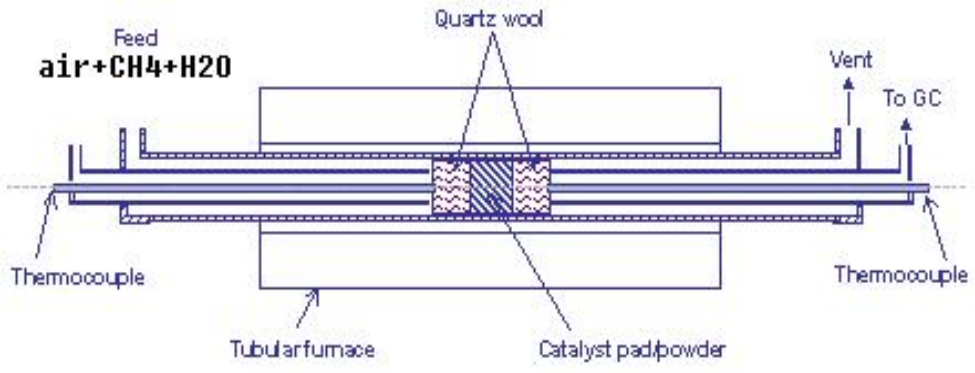

Figure 3.1 Sketch of the microreactor

Figure 3.2 Photo of testing system

Figure 3.3 Catalyst samples, 150, 80, 15 g/ft^3 (left to right)

was recorded on the computer as a reaction parameter was from TC1, and TC2 was connected to the temperature controller for adjustment and stabilization. These two temperatures were not very close to each other, usually plus or minus twenty degree at most. TC3 was between the inside of the oven and the outside of the tube and was attached to the surface of the tube, hence its temperature was always a little lower than that of TC1 and TC2. It is used as a monitor in case of any malfunction in TC1 or TC2. Pressure drop in the reactor was also recorded by a pressure gauge to see if the catalysts blocked the gas flows. Finally, at the outlet of the reactor, part of the exhausted gas was imported to a gas chromatograph (GC) for analysis. This GC is HP 5890 A type with a 80/100 HAYESEP Q column from Supelco, and the flow rate of carrier gas was set at 18.5 mL/min.

Gas and Water Supply: All the gases used in this study were purchased from Praxair in high pressure cylinders. The gases used were: 10 % methane in nitrogen mixture (pure methane was used instead of methane-nitrogen mixture for a short time at the very beginning of the project), hydrogen (Ultrahigh purity, UHP, 5.0), nitrogen (UHP 5.0), helium (carrier gas for the GC, UHP 5.0) and dry air (extra dry). The feed to the reactor consisted of methane nitrogen mixture and air with the addition of water during some of the runs. Gas feeds mixed with each other at the inlet of the reactor. Two gas supply lines, both with a flow meter, were used, line one for air only, and line two for methane, hydrogen and nitrogen, but these three gases were used at different times, so at anytime there would be only one gas in line two. Additional water (liquid reverse osmosis water) was introduced and controlled, if needed, by a syringe pump (5 mL in volume) into the inlet of the reactor where water was vaporized by a heat gun and taken into the reactor by other gas feeds. The flow meter for air flow is Matheson Modular DYNA – Blender model 8250, and that for hydrogen is AALBORG Mass Flow Controller GFC 17. Both of the flow meters were calibrated before using.

3.2 Experiment procedures

It is important to mention that the following parameters and procedures were fixed after the exploratory tests, which were done to find the best experimental conditions for the repeatability and reproducibility of the experiments. Therefore when exploratory tests are discussed in next chapter (Chapter 4. Results and Analysis), their conditions and procedures will be given individually. For detailed information, see the run list in Appendix A.

3.2.1 Reactant Compositions

The flow rate of air was first fixed at 99±1.5 mL/min in exploratory runs and then doubled to 198±1.5 mL/min, and the flow rate of the 10% methane stream was adjusted so that the methane concentration was 3100±100, 4700±150 and 8500±300 ppm. When water was added to the feed, it was added at a rate of 0.5 mL/h; this resulted in a feed mixture with 5% mole water on dry basis. Experiments were done using different catalyst samples with different Pd loadings. A list of the experiments is given in Appendix A.

3.2.2 Ignition and extinction curves of methane combustion

The purpose of these tests was to gain understanding of the effects of experimental conditions on the ignition and extinction behavior of catalytic methane oxidation. The experimental factors studied were catalyst pretreatment, reaction temperature, methane concentration, additional water presence and Pd loading. A series of preliminary experiments were done to determine procedures which resulted in reproducible results. It was found that a high temperature pretreatment was required to obtain reproducible results. The procedures established for ignition-extinction experiments which yielded reproducible results are described below.

a. Reduction pretreatment: This was done before all the experiments except some of the exploratory runs to produce the same initial states. The temperature of the reactor was first raised to 370℃, at which H_2 flow was started. Then the temperature was increased to 570℃ to reduce the catalysts. This step took 15 minutes. After that the H_2 flow was cut off. And the catalyst was cooled down in H_2 atmosphere until the temperature reached 200℃ or 300℃.

b. Ignition: CH_4 flow was started, and after one minute air flow was started. The temperature would usually increase rapidly by 10-20℃ before falling again. When the temperature stabilized, the product gas analysis was started, after which the set temperature was increased by 40-50℃ to proceed to another test. This process was continued until the conversion of methane achieved 100 %;

c. Extinction: repeated step b reversely, i.e., decreasing the temperature instead of rising to analyze the reaction at different temperature. This step and the whole experiment ended at the temperature region where the ignition started.

3.2.3 Reduction and oxidation

It is known that the oxidation state of Pd affects the rate of methane oxidation. To examine this effect, conversions of methane as a function of temperature were measured after reduction and oxidation pretreatment. These tests offered a comparison of the activity of different Pd phases, including reduced state, oxidized state and after-ignition state.

a. Reduction pretreatment: The procedure was the same as Step a in Section 3.2.2 and would lead to reduced surface states on the catalysts.

b. Oxidation pretreatment (optional): The temperature was and kept at 520℃. When reactor temperature reached this stage, air flow was started. Catalysts would be heated under this condition for 1 hour – 5 hours, depending on different experiments. This step would produce oxidized Pd states on the catalysts and hence was skipped in reduction-only experiments;

c. Extinction: The temperature was increased to 600℃, or reduced to 400℃ depending on different catalyst samples, then followed step c in section 2.2;

3.2.4 Catalysts' performance at high temperature

a. Thermal decomposition: Nitrogen was flowed through the reactor at temperature of 870℃, so that the transformation of PdO to Pd would occur. This treatment was done for 2.5 hours.

b1. Cooling down and extinction test: The temperature of the reactor was reduced to 450℃ for extinction test, then followed step c in section 3.2.2; or:

b2. Extinction test at high temperature: The temperature of the reactor was reduced to 800℃, then followed step c in section 3.2.2. As stated in the literature, a fluctuation of methane conversion took place at 750 – 700℃.

3.3 Catalyst Characterization

Characterization tests are essential to obtain a further understanding on the compositions of the catalyst samples. Two analytic methods were employed: neutron activation analysis and X-ray diffraction.

3.3.1 Instrumental Neutron Activation Analysis (INAA)

Neutron activation analysis is a technique for determining the elemental composition. It is one of the most accurate methods for determining the

composition of solids. In this work, INAA was used to measure the concentrations of Pd and lanthanum in catalysts with different Pd loadings. Six samples, two from each of the three types of catalysts, were sent to the Slowpoke Nuclear Reactor Facility at the University of Alberta for INAA analysis.

3.3.2 X-Ray Diffraction (XRD)

Samples with a Pd loading of 150 g/ft^3 were examined by wide angle x-ray diffraction. A Philips x-ray diffractometer with a PW1730/10 x-ray generator, a PW1050/70 vertical goniometer, a PW1965/60 detector, a copper anode and Amray Model E3-202 GVW-774 graphite monochrometer were used.

Six samples were examined by XRD. All samples were examined as finely ground powders. The first three samples were: Untreated (fresh as received from the producer), reduced (with hydrogen pretreatment, procedures given in Part a, Section 3.2.2 in this chapter) and oxidized (with hydrogen pretreatment first and then oxidation pretreatment, procedures given in Part a, Section 2.2 and Part b, Section 2.3 in this chapter). The next three samples were obtained by scraping the washcoat from the monolith support. This was done to increase the Pd concentration in the samples; all the Pd is present in the washcoat. XRD patterns were recorded over the 10 - 60 °2θ range in the step scan mode. The step size was 0.05 °2θ per step at a step time of 4 s. One scan was done at 40 s per step.

Chapter 4 Results and Analysis

4.1 Preliminary tests

At the beginning of the study, a variety of experiments were performed. These experiments had two goals: 1.Getting a general idea of the catalysts' behavior; 2. Finding proper pretreatments to make the catalysts' behavior reproducible, and the catalysts would have same initial states so that subsequent comparisons would be meaningful. The procedures and experimental conditions were hence a little different than what was listed in Chapter 3. Catalyst sample 4 (run number begins with 4, see Table 4.1 on Page 30, or Appendix A) was used for these tests. The original mass of this sample was 1.20 g; however, some of the catalysts were lost during a change of reactor. So the real mass of this sample is unknown. But this will not affect the general trends derived from these tests, because the same mass was used in all runs.

4.1.1 Tests without any pretreatments

To obtain a preliminary understanding of these catalysts, exploratory tests were first done on fresh samples as received from the manufacturer, i.e. no pretreatment was involved. Fig. 4.1 to 4.3 give typical results from two continuous cycles on not aged catalyst samples with no pretreatment. The initial temperature was around 300°C, and then raised stepwise by 50°C increments with one or two steady-state tests at every temperature stage (the reactions were believed to reach steady states when temperature oscillation inside the reactor was less than one degree within the last five minutes). After the conversion reached 100%, the reactor was cooled gradually by 50°C increments with tests at each step, until the final temperature reached 300°C, or the conversion was lower than 10%. It can be seen that these results share the same S-shape, and the light-off temperature are all around 400°C. But their specific behaviors are highly different. In Fig. 4.1, conversion in the

extinction stage is higher than that in the ignition stage, forming a classic conversion hysteresis. In contrast, in Fig. 4.3 conversion in the ignition stage is higher, while in Fig. 4.2 there is a crossover for these two conversion curves. Furthermore, the complete conversion temperatures (temperature at which all the methane is combusted) from three figures are also different. In conclusion, these results are not reproducible, and it is probable that the catalyst surface was changing.

List of runs for methane oxidation[a]								
Run #	**Catalyst, g/ft^3**	**Procedure[b]**	**Reduction**	**Oxidation**	**CH_4, mL/min**	**CH_4, ppm**	**T, °C**	**Water, 5% mol**
401-425	150	exploratory runs			9.75	4700± 150	-	N
426	150	I	15 min	N	9.75	4700± 150	300~ 450	N
427	150	I-E	-	-	9.75	4700± 150	450~ 300	N
428	150	I	15 min	N	9.75	4700± 150	300~ 450	N
429	150	I-E	-	-	9.75	4700± 150	450~ 300	N
430	150	I	15 min	N	9.75	4700± 150	300~ 450	N
431	150	I-E	-	-	9.75	4700± 150	450~ 300	N
432	150	E	15 min	520°C, 2.5 h	9.75	4700± 150	500~ 300	N
433	150	E	15 min	520°C, 2.5 h	9.75	4700± 150	500~ 300	N
434	150	E	15 min	450°C, 2.5 h	9.75	4700± 150	500~ 300	N
435	150	E	15 min	450°C,1 h	9.75	4700± 150	500~ 300	N
436	150	E	15 min	450°C, 15 min	9.75	4700± 150	500~ 300	N
437	150	E	15 min	520°C, 5 h	9.75	4700± 150	500~ 300	N
438	150	E	N2/870°C/ 2.5h	N	9.75	4700± 150	500~ 300	N
439	150	E	N2/870°C/ 2.5h	N	9.75	4700± 150	850~ 300	N
440	150	E	N2/870°C/ 2.5h	N	9.75	4700± 150	850~ 300	N
501	80	I	15 min	N	9.75	4700± 150	300~ 450	N

Run #	Catalyst, g/ft^3	Procedure[b]	Reduction	Oxidation	CH_4, mL/min	CH_4, ppm	T, °C	Water, 5% mol
502	80	I-E	-	-	9.75	4700± 150	450~ 300	N
503	80	E	15 min	N	9.75	4700± 150	500~ 300	N
504	80	E	15 min	N	9.75	4700± 150	500~ 300	N
505	80	I	15 min	N	9.75	4700± 150	200~ 400	N
506	80	I-E	-	-	9.75	4700± 150	400~ 200	N
507	80	I	N	N	9.75	4700± 150	200~ 450	N
508	80	I-E	-	-	9.75	4700± 150	450~ 200	N
509	80	E	15 min	N	9.75	4700± 150	400~ 250	N
510	80	E	15 min	520°C, 5 h	9.75	4700± 150	450~ 250	N
511	80	E	15 min	520°C, 1 h	9.75	4700± 150	400~ 200	N
601	15	I	15 min	N	9.75	4700± 150	300~ 600	N
602	15	I-E	-	-	9.75	4700± 150	600~ 300	N
603	15	I	15 min	N	9.75	4700± 150	300~ 600	N
604	15	I-E	-	-	9.75	4700± 150	600~ 300	N
605	15	I	15 min	N	9.75	4700± 150	300~ 600	N
606	15	I-E	-	-	9.75	4700± 150	600~ 300	N
607	15	E	15 min	N	9.75	4700± 150	600~ 300	N
608	15	I	15 min	N	19.75	8500± 300	300~ 600	N
609	15	I-E	-	-	19.75	8500± 300	600~ 300	N

Run #	Catalyst, g/ft^3	Procedure[b]	Reduction	Oxidation	CH_4, mL/min	CH_4, ppm	T, °C	Water, 5% mol
610	15	I	15 min	N	6.00	3100± 100	300~ 600	N
611	15	I-E	-	-	6.00	3100± 100	600~ 300	N
612	15	E (D)	15 min	N	9.75	4700± 150	600-480(2h)300 N	
613	15	E	15 min	520°C, 5 h	9.75	4700± 150	600~ 300	N
614	15	E	15 min	520°C, 5 h	19.75	8500± 300	600~ 300	N
615	15	E	15 min	520°C, 5 h	6.00	3100± 100	600~ 300	N
616	15	E	15 min	520°C, 1 h	9.75	4700± 150	400~ 200	N
617	15	E	15 min	520°C, 2 h	9.75	4700± 150	400~ 200	N
701	150	I	Y, 15 min	N	9.75	4700± 150	200~ 350	N
702	150	I-E	-	-	9.75	4700± 150	350~ 200	N
703	150	E	15 min	N	9.75	4700± 150	400~ 200	N
704	150	E	15 min	520°C, 5 h	9.75	4700± 150	400~ 200	N
705	150	I	15 min	N	19.75	8500± 300	200~ 200	N
706	150	I-E	-	-	19.75	8500± 300	400~ 200	N
707	150	E	15 min	N	19.75	8500± 300	400~ 200	N
708	150	E	15 min	N	19.75	8500± 300	400~ 200	N
709	150	I	15 min	N	6.00	3100± 100	200~ 300	N
710	150	I-E	-	-	6.00	3100± 100	300~ 200	N
711	150	E	15 min	N	6.00	3100± 100	400~ 200	N

Run #	Catalyst, g/ft^3	Procedure[b]	Reduction	Oxidation	CH_4, mL/min	CH_4, ppm	T, °C	Water, 5% mol
712	150	E	15 min	520°C, 5 h	6.00	3100± 100	400~ 200	N
801	150	I	15 min	N	9.75	4700± 150	200~ 350	Y
802	150	I-E	-	-	9.75	4700± 150	350~ 200	Y
803	150	I	15 min	N	9.75	4700± 150	200~ 550	Y
804	150	I-E	-	-	9.75	4700± 150	550~ 200	Y
805	150	I	45 min	N	9.75	4700± 150	200~ 550	Y
806	150	I-E	-	-	9.75	4700± 150	550~ 200	Y
807	150	E	135 min	N	9.75	4700± 150	400~ 200	Y
808[c]	150	I	75 min	520°C, 5 h	9.75	4700± 150	200~ 550	Y
809	150	I-E	-	-	9.75	4700± 150	550~ 200	Y
810	150	I	75 min	N	9.75	4700± 150	200~ 550	Y
811	150	I-E	-	-	9.75	4700± 150	550~ 200	Y
901	150	I	15 min	N	9.75	4700± 150	200~ 400	Y
902	150	I-E	-	-	9.75	4700± 150	400~ 300	Y
903	150	I	15 min	N	9.75	4700± 150	200~ 400	Y
904	150	I-E	-	-	9.75	4700± 150	400~ 300	Y
905	150	I	15 min	N	9.75	4700± 150	200~ 500	Y
906	150	I-E	-	-	9.75	4700± 150	500~ 300	Y

Run #	Catalyst, g/ft^3	Procedure[b]	Reduction	Oxidation	CH_4, mL/min	CH_4, ppm	T, °C	Water, 5% mol
907[c]	150	I	15 min	520°C, 5 h	9.75	4700± 150	200~ 600	Y
908	150	I-E	-	-	9.75	4700± 150	600~ 300	Y
909	150	I	15 min	N	9.75	4700± 150	200~ 600	Y
910	150	I-E	-	-	9.75	4700± 150	600~ 300	Y
911	150	I	15 min	N	9.75	4700± 150	200~ 500	Y
912	150	I-E	-	-	9.75	4700± 150	500~ 300	Y
913	150	I	N	N	9.75	4700± 150	200~ 600	Y
914	150	I-E	-	-	9.75	4700± 150	600~ 400	Y
915	150	I	N	N	9.75	4700± 150	200~ 650	Y
916	150	I-E	-	-	9.75	4700± 150	650~ 400	Y
917	150	I	N	N	9.75	4700± 150	200~ 650	Y
918	150	D	N	N	9.75	4700± 150	585, 17 h	Y
919	150	D	N	N	9.75	4700± 150	585, 25 h	Y
920	150	-	-	-	-	-	-	-
921	150	I	N	N	9.75	4700± 150	200~ 600	N
922	150	I-E	-	-	9.75	4700± 150	600~ 360	N
923	150	I	N	N	9.75	4700± 150	200~ 600	N
924	150	I-E	-	-	9.75	4700± 150	600~ 350	N
925	150	I	N	N	9.75	4700± 150	200~ 650	N
926	150	I-E	-	-	9.75	4700± 150	650~ 350	N

Run #	Catalyst, g/ft^3	Procedure[b]	Reduction	Oxidation	CH_4, mL/min	CH_4, ppm	T, °C	Water, 5% mol
927	150	I	15 min	N	9.75	4700± 150	200~ 550	N
928	150	I-E	-	-	9.75	4700± 150	550~ 300	N
929	150	I	15 min	N	9.75	4700± 150	200~ 550	N
930	150	I-E	-	-	9.75	4700± 150	550~ 300	N
931	150	D	N	N	9.75	4700± 150	585, 29 h	stop at 24 h
932	150	D	N	N	9.75	4700± 150	585, 60 h	stop at 51 h
933	150	after 932, D	N	N	9.75	4700± 150	585, 5 h	N
Note:								
[a]. The flow rate of air was fixed at 198.00 mL/min. The mass of catalyst samples for all the runs								
was 1.20 g, except for Run# 04XX, some catalysts were lost.								
[b]. I=ignition, E=extinction, I-E=extinction after ignition, D=deactivation								
[c]. Oxidation was done before reduction.								

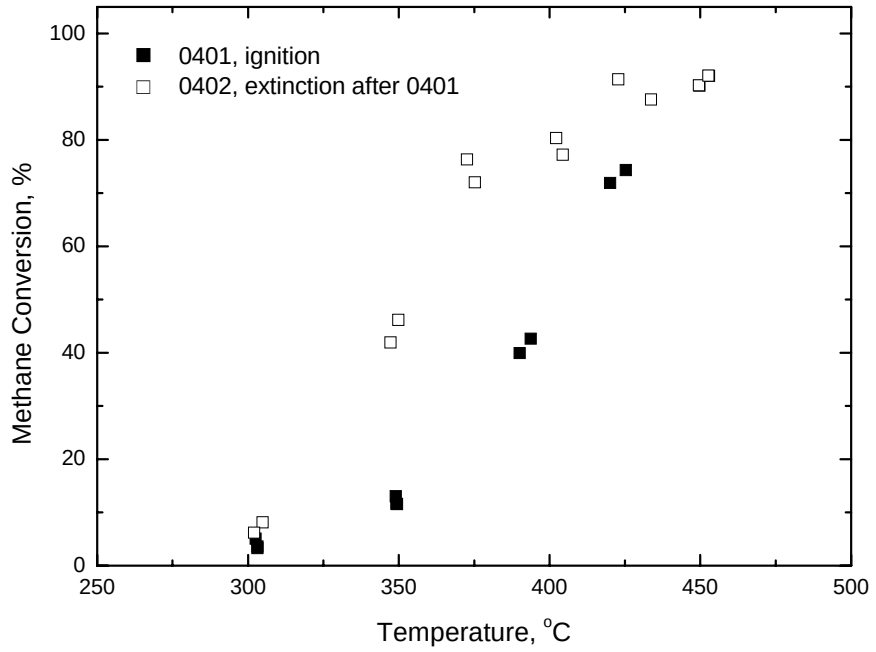

Figure 4.1 Ignition and extinction curves of methane combustion Run#: 0401, 0402; Cat. = Pd wash coat catalysts, 150 g/ft^3, <1.20 g, not aged; CH_4 = 10% methane in nitrogen, 4.7±0.1 mL/min, 4700±150 ppm; Air = 99±1.5 mL/min

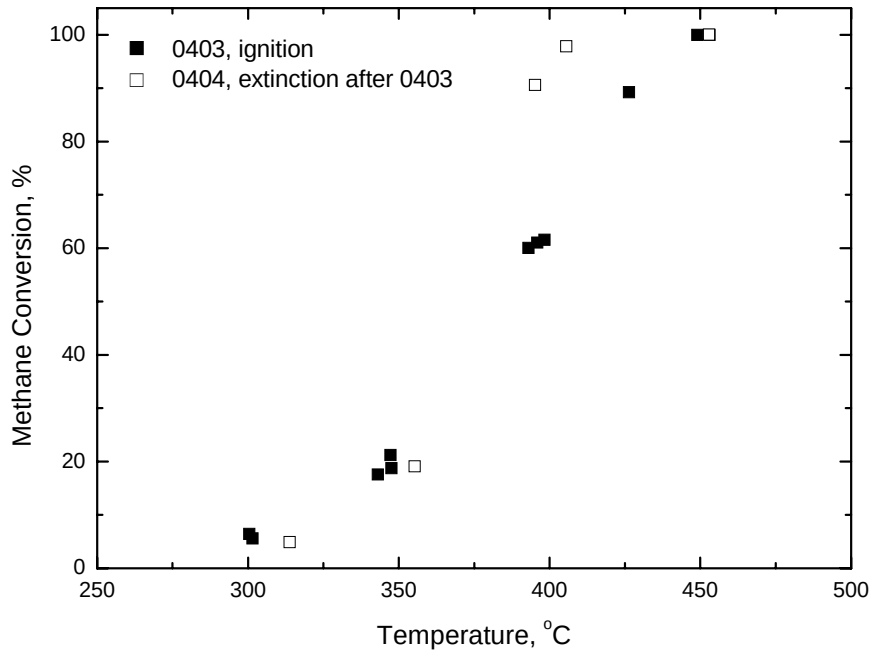

Figure 4.2 Ignition and extinction curves of methane combustion Run#: 0403, 0404;Cat. = Pd wash coat catalysts, 150 g/ft^3, <1.20 g, not aged CH_4 = 10% methane in nitrogen, 4.7±0.1 mL/min, 4700±150 ppm; Air = 99±1.5 mL/min

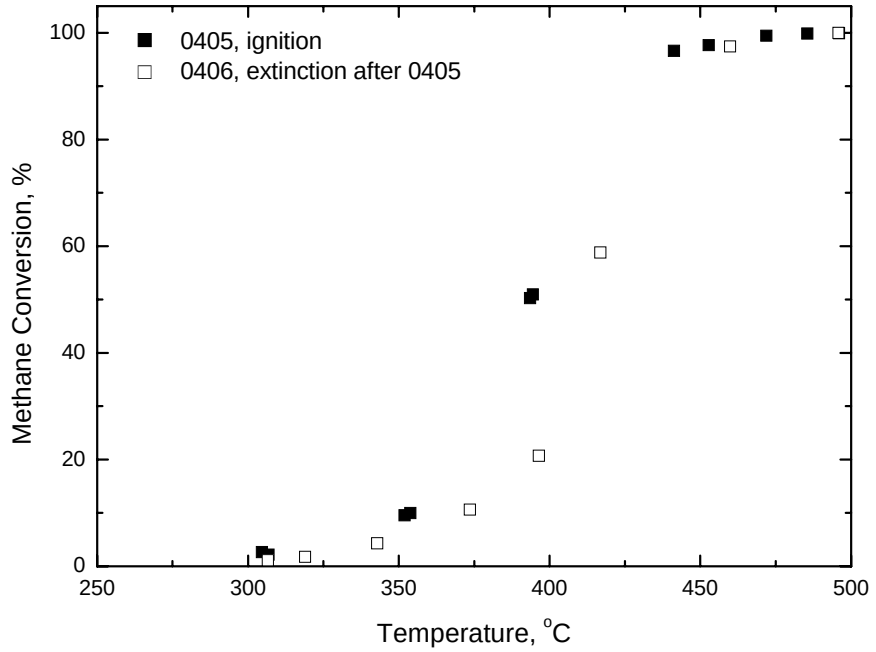

Figure 4.3 Ignition and extinction curves of methane combustion Run#: 0405, 0406; Cat. = Pd wash coat catalysts, 150 g/ft^3, <1.20 g, not aged CH_4 = 10% methane in nitrogen, 4.7±0.1 mL/min, 4700±150 ppm; Air = 99±1.5 mL/min

4.1.2 Tests with ageing pretreatments

Ageing, or high temperature pretreatment in air, is reported in much of the literature and can often stabilize catalysts performance to some extent. Usually Umicore, the manufacturer of these catalysts, suggests an ageing process to produce stable catalysts, and thus it was employed as a potential solution to get reproducible results. A new series of experiments was then performed. The catalyst sample was heated for eight hours in air flow at 600°C for only once as described in Chapter 3. The flow rates of both air and methane mixture were doubled compared with former runs for better simulation of the outlet gases from natural gas engines. Results from test after ageing, in the form of ignition and extinction curves are given in Fig. 4.4 to 4.8.

The catalyst activities seem to be lower than those shown in Fig. 4.3, which could be attributed to the increase of flow rate. Meanwhile, from Fig. 4.4 to 4.6, it seems that the catalysts gradually lost some of their activity, shown by the moving of the curves toward right hand side. This observation was not accidental and is discussed later. Most importantly, catalysts' behaviours, especially these on extinction stages, did become slightly more stable with a small change in light-off temperatures. But in Fig. 4.7, under the same reaction conditions, the activity of the catalyst was higher, and the shapes of ignition and extinction curves in this figure were also different with those in the former three figures. Then in Fig. 4.8, the catalyst activities again were lower. These non-reproducible results were not acceptable, and other methods, such as hydrogen pretreatment, were then tried to achieve reproducibility.

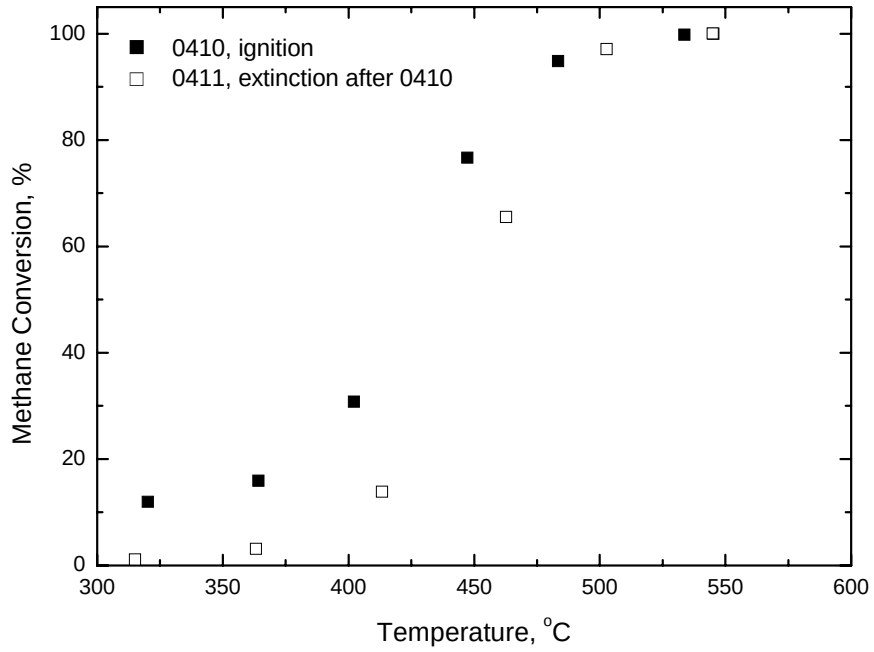

Figure 4.4 Ignition and extinction curves of methane combustion Run#: 0410, 0411; Cat. = Pd wash coat catalysts, 150 g/ft^3, <1.20 g, aged CH_4 = 10% methane in nitrogen, 9.5±0.2 mL/min, 4700±150 ppm; Air = 198±1.5 mL/min

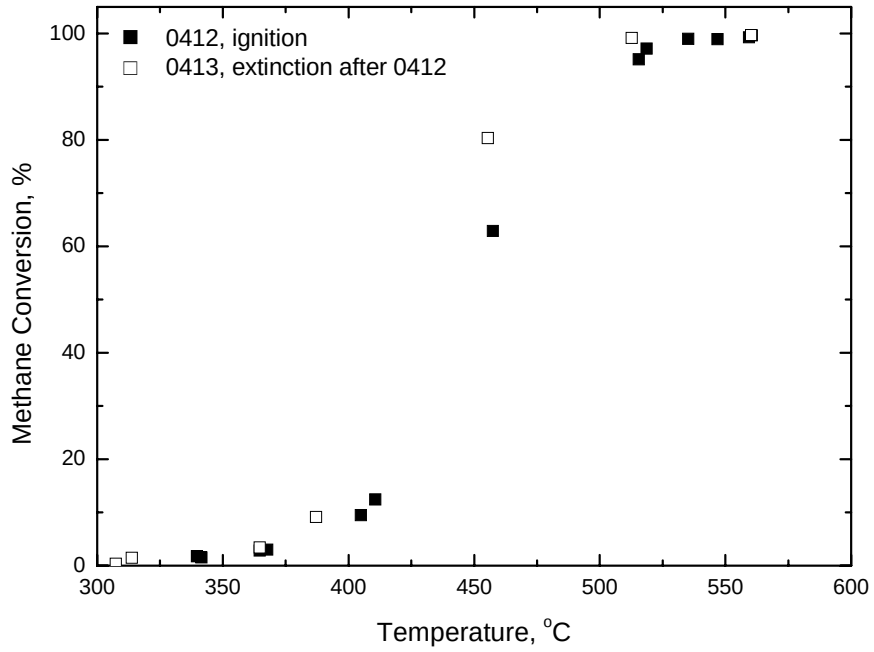

Figure 4.5 Ignition and extinction curves of methane combustion Run#: 0412, 0413; Cat. = Pd wash coat catalysts, 150 g/ft^3, <1.20 g, aged CH_4 = 10% methane in nitrogen, 9.5±0.2 mL/min, 4700±150 ppm; Air = 198±1.5 mL/min

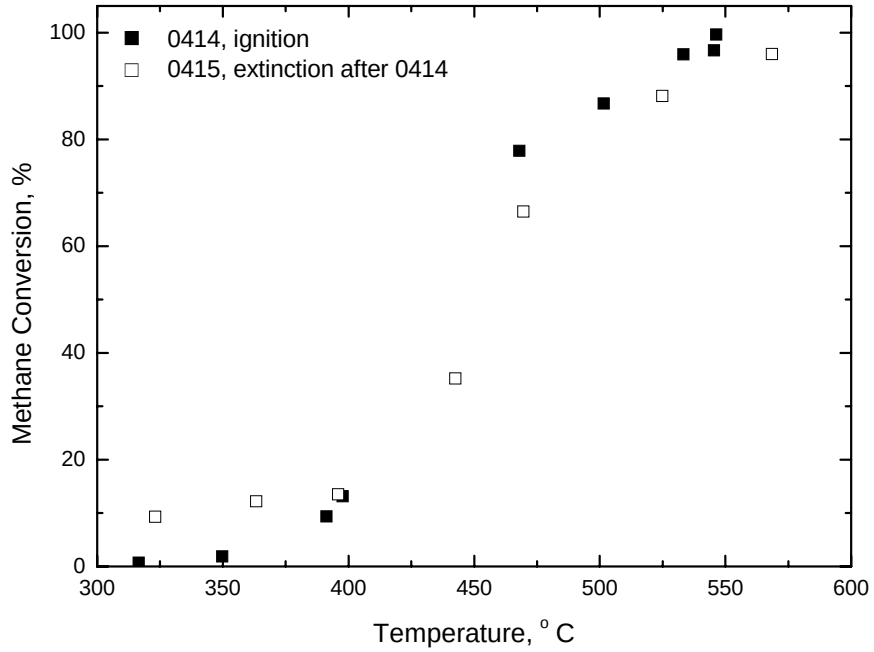

Figure 4.6 Ignition and extinction curves of methane combustion Run#: 0414, 0415; Cat. = Pd wash coat catalysts, 150 g/ft^3, <1.20 g, aged CH_4 = 10% methane in nitrogen, 9.5±0.2 mL/min, 4700±150 ppm; Air = 198±1.5 mL/min

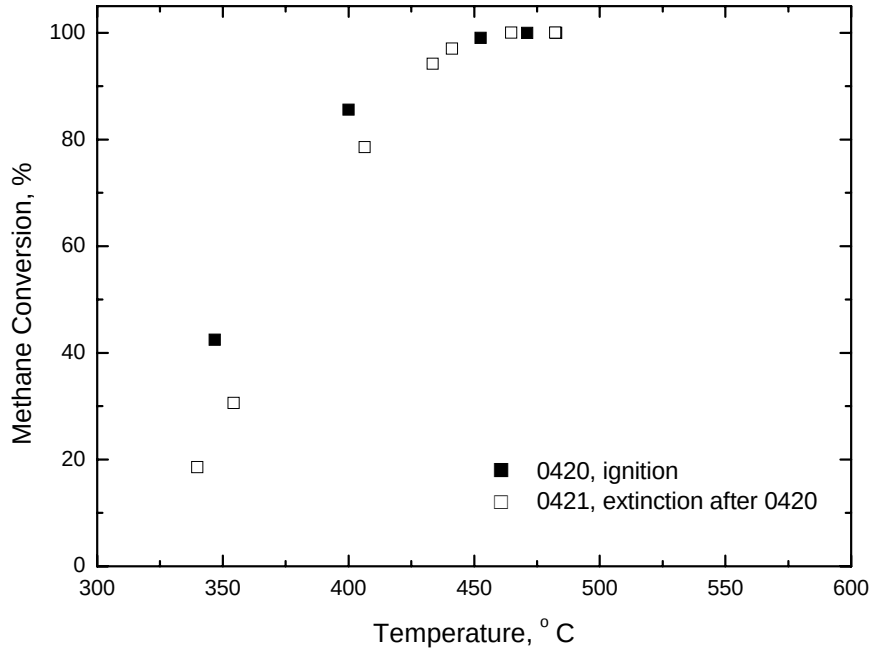

Figure 4.7 Ignition and extinction curves of methane combustion Run#: 0400, 0421; Cat. = Pd wash coat catalysts, 150 g/ft^3, <1.20 g, aged CH_4 = 10% methane in nitrogen, 9.5±0.2 mL/min, 4700±150 ppm; Air = 198±1.5 mL/min

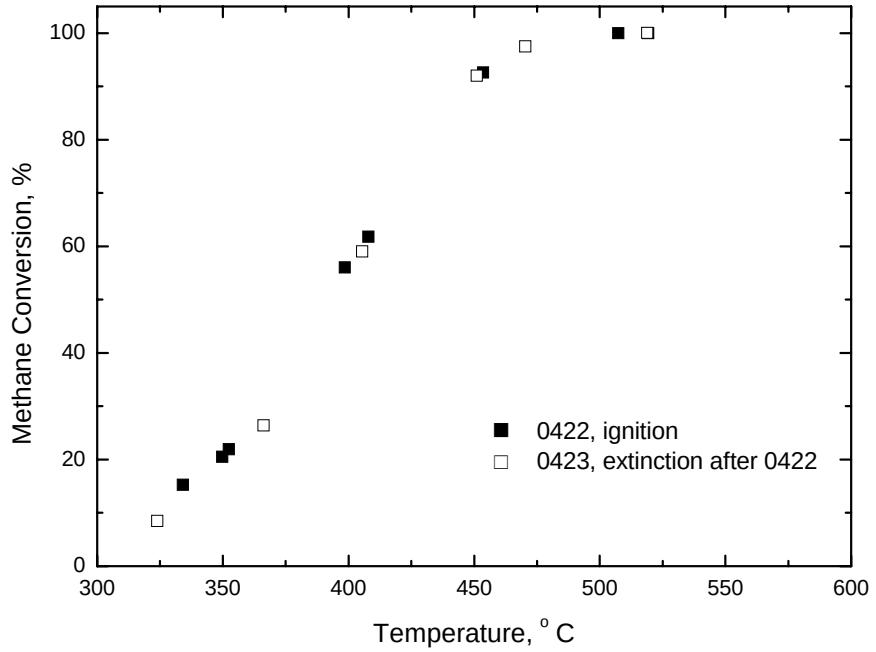

Figure 4.8 Ignition and extinction curves of methane combustion Run#: 0422, 0423; Cat. = Pd wash coat catalysts, 150 g/ft^3, <1.20 g, aged CH_4 = 10% methane in nitrogen, 9.5±0.2 mL/min, 4700±150 ppm; Air = 198±1.5 mL/min

4.1.3 The effects of reduction pretreatments

Hydrogen pretreatments, or reduction, was performed, following the same procedure given in Chapter 3. The temperature of the reactor was first raised to 370℃, and then H_2 flow was started. Then the temperature was increased to 570℃ to reduce the catalysts. This step took 15 minutes. After that the H_2 flow was stopped and the reactor allowed to cool.

The same procedures for the ignition and extinction tests were repeated. The results from reduced samples are given in Fig. 4.9, 4.10 and 4.11. Two things are obvious from these figures. First of all, the performance of the catalysts, especially the performance in the ignition stages, are very similar to each other, proving that reduction pretreatment stabilized the activity of the catalyst sample. Secondly, the reduction increased the activity of the catalysts. The light-off temperature decreased from around 400℃ to 350℃, and all the methane was converted at about 425℃. This is consistent with many observations in the literature (see Chapter 2). To sum up, hydrogen pretreatment has a positive impact on the activity of catalysts, and most importantly was able to give a common starting point for kinetic experiments.

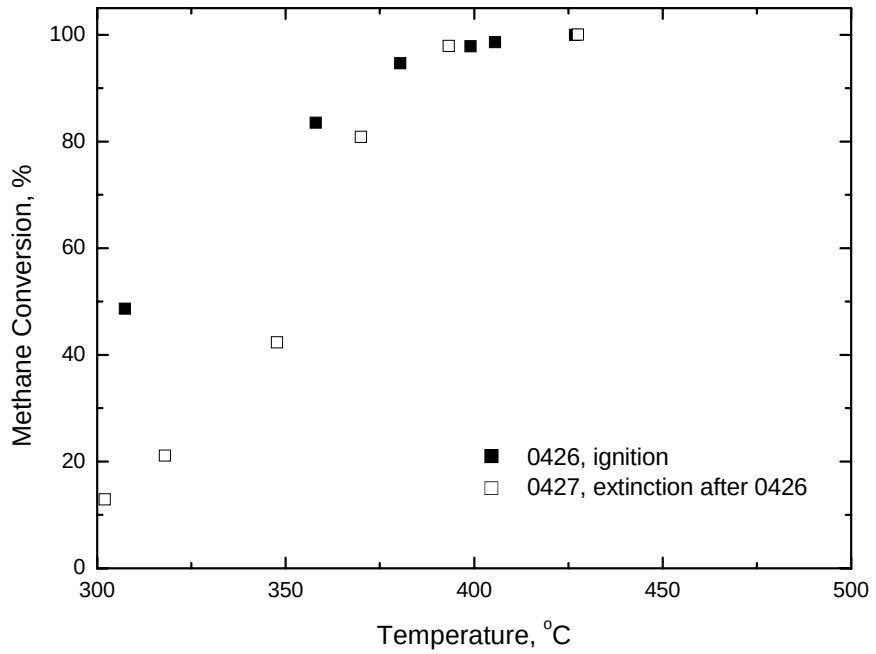

Figure 4.9 Ignition and extinction curves of methane combustion Run#: 0426, 0427; Cat. = Pd wash coat catalysts, 150 g/ft^3, <1.20 g, aged and reduced; CH_4 = 10% methane in nitrogen, 9.5±0.2 mL/min, 4700±150 ppm; Air = 198±1.5 mL/min

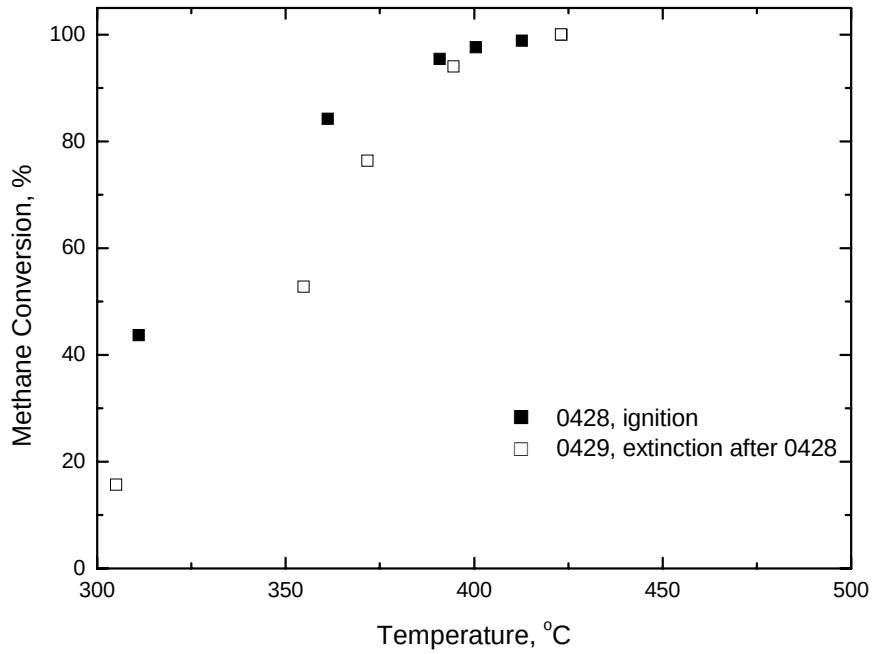

Figure 4.10 Ignition and extinction curves of methane combustion Run#: 0428, 0429; Cat. = Pd wash coat catalysts, 150 g/ft^3, <1.20 g, aged and reduced; CH_4 = 10% methane in nitrogen, 9.5±0.2 mL/min, 4700±150 ppm; Air = 198±1.5 mL/min

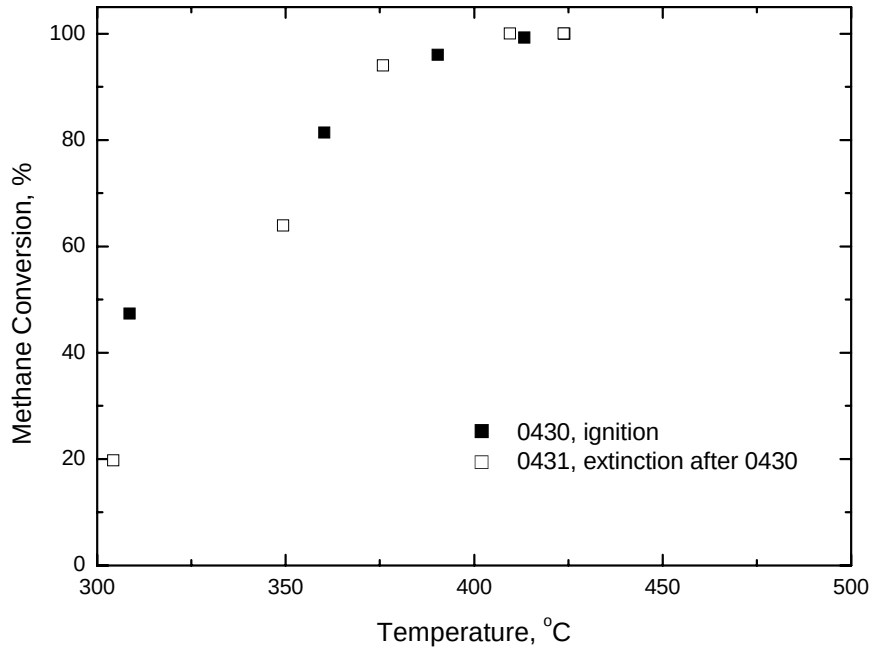

Figure 4.11 Ignition and extinction curves of methane combustion Run#: 0430, 0431; Cat. = Pd wash coat catalysts, 150 g/ft^3, <1.20 g, aged and reduced; CH_4 = 10% methane in nitrogen, 9.5±0.2 mL/min, 4700±150 ppm; Air = 198±1.5 mL/min

4.2 Ignition and Extinction Curves

Once the preliminary experiments were completed, and an understanding of the catalyst behaviour thus obtained, a series of experiments were conducted. The goal of these experiments was to understand the general ignition and extinction patterns of catalytic methane combustion on this type of Pd catalysts. They were done on three catalysts with Pd loadings of 15, 80 and 150 g/ft^3 under a variety of conditions to determine the influence of reaction temperature, methane concentration, additional water presence and Pd loading. The initial temperature was around 200 or 300°C, depending on different catalyst samples, and then raised by 50°C after two steady state tests at every temperature stage. After the conversion reached 100%, the reactor would be cooled down gradually also by 50°C increments with tests at each step, until the final temperature arrived at 300°C, or the conversion was lower than 10%.

4.2.1 Unusual trend of ignition and extinction curves

Fig. 4.12 to 4.16 show the effect of Pd loading of constant methane concentration. First and foremost, the general trends of ignition and extinction here were different from the traditional light off curves. Their activities both grow with temperatures and show S-shape increase. But contrary with the hysteresis in traditional cases, i.e. extinction braches are more active than ignition curves, all these experiments on different catalyst samples had ignition curves have higher or equal conversion than extinction curves. This phenomenon is particularly interesting because it is rarely seen in previous literature or even former research on the similar catalysts (Litto 2008). Firstly, it may attribute the harm of water on the catalysts. Water has been known as one of the important poisons on Pd catalysts. In this case, as a result, catalysts which had been used in ignition stages might lose some activity due to the exposure to water, causing the decreasing of methane conversion in extinction branches. Another preliminary explanation is the temperature distribution

inside of the reactor. Litto (2008) investigated the temperature distribution inside of the monolith reactor by eight thermocouples, and discovered that the upstream temperature was usually higher than that of downstream at ignition stages, whilst, as mentioned above, the temperature used in this project is further downstream, and is probably not the “real” temperature on the catalysts, so one has to be careful when analyzing this because the activity significantly relies on the temperature profile inside of the reactor. Also, it is seen that the higher metal loading gives a higher catalyst activity, which is expected. Better and detailed investigation would be possible if a general profile of the temperature distribution in the reactor was available.

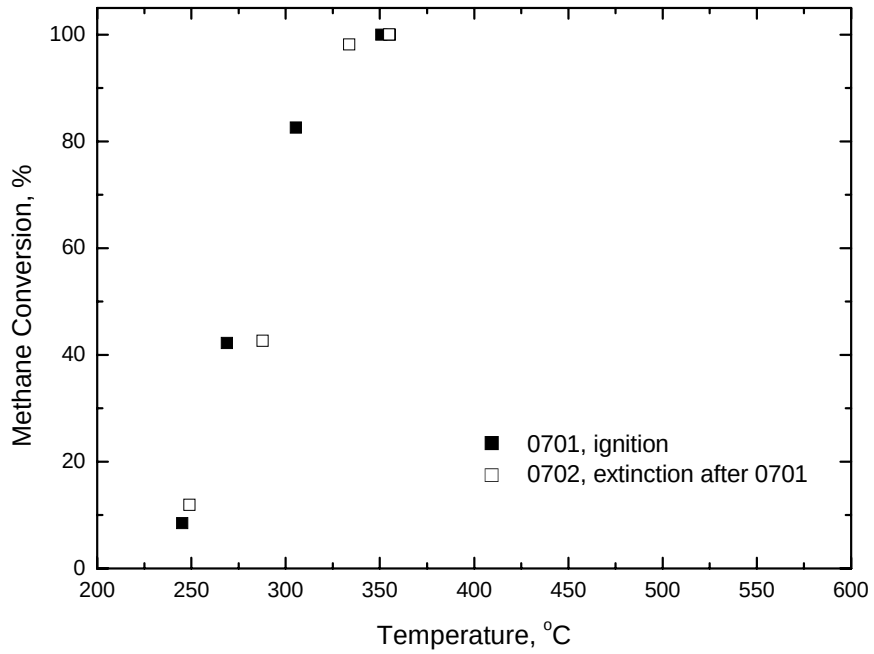

Figure 4.12 Ignition and extinction curves of methane combustion Run#: 0701, 0702; Cat. = Pd wash coat catalysts, 150 g/ft^3, 1.20 g, aged and reduced; CH_4 = 10% methane in nitrogen, 9.5±0.2 mL/min, 4700±150 ppm; Air = 198±1.5 mL/min

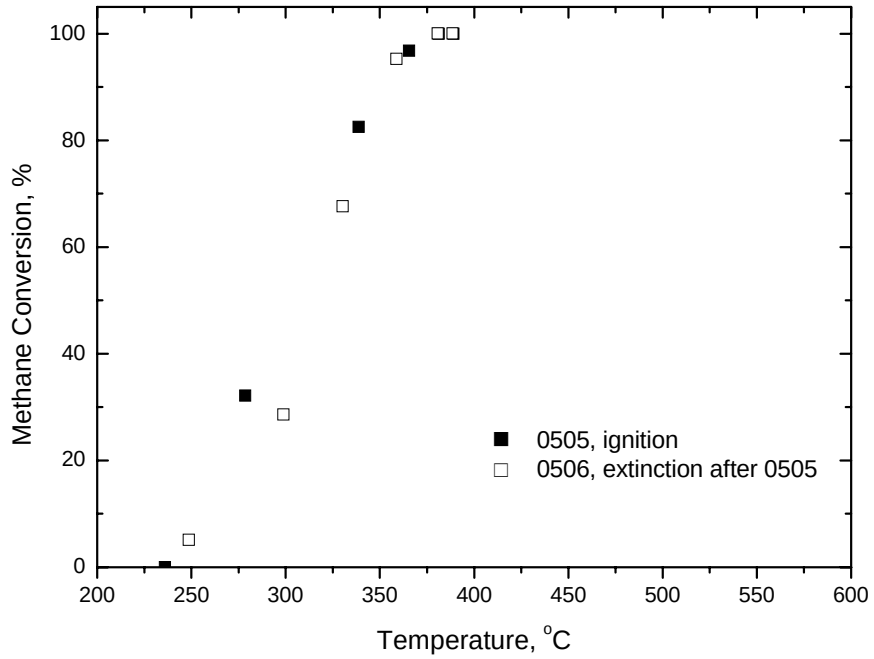

Figure 4.13 Ignition and extinction curves of methane combustion Run#: 0506, 0507; Cat. = Pd wash coat catalysts, 80 g/ft^3, 1.20 g, aged and reduced; CH_4 = 10% methane in nitrogen, 9.5±0.2 mL/min, 4700±150 ppm; Air = 198±1.5 mL/min

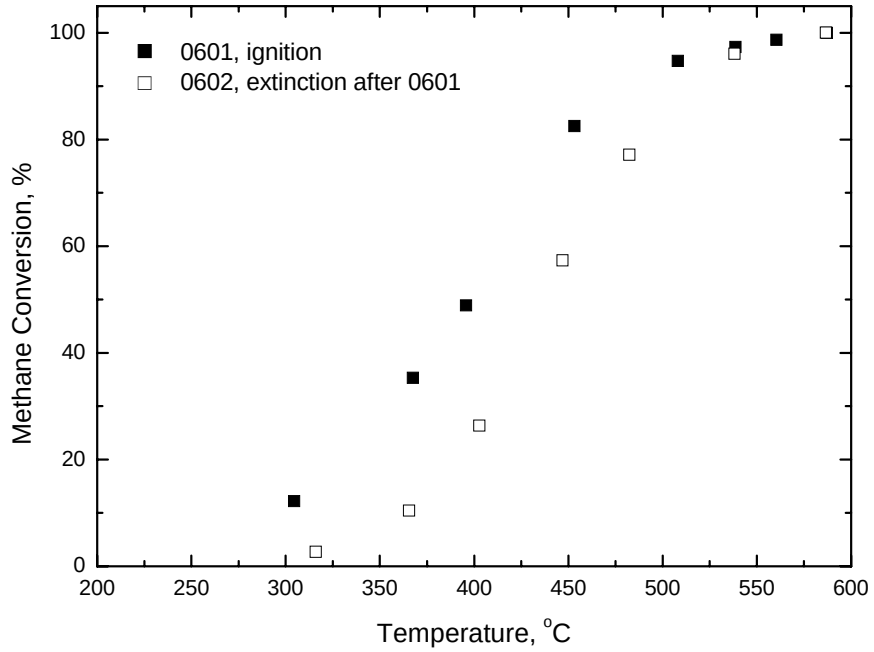

Figure 4.14 Ignition and extinction curves of methane combustion Run#: 0601, 0602; Cat. = Pd wash coat catalysts, 15 g/ft^3, 1.20 g, aged and reduced; CH_4 = 10% methane in nitrogen, 9.5±0.2 mL/min, 4700±150 ppm; Air = 198±1.5 mL/min

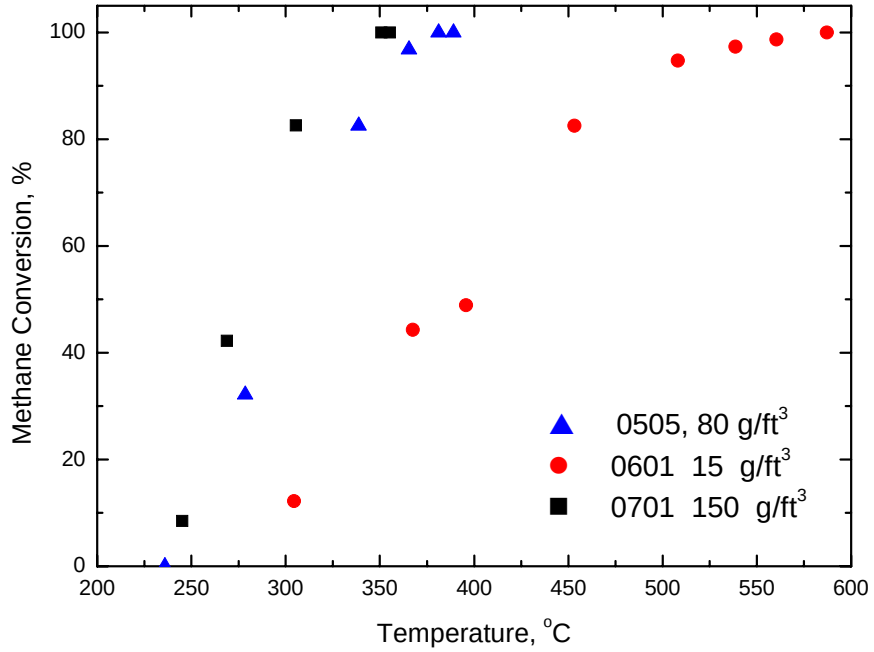

Figure 4.15 Comparison among ignition curves of Pd loadings; Run#: 0505, 0601, 0701; Cat. = Pd wash coat catalysts, 1.20 g, aged and reduced CH_4 = 10% methane in nitrogen, 9.5±0.2 mL/min, 4700±150 ppm; Air = 198±1.5 mL/min

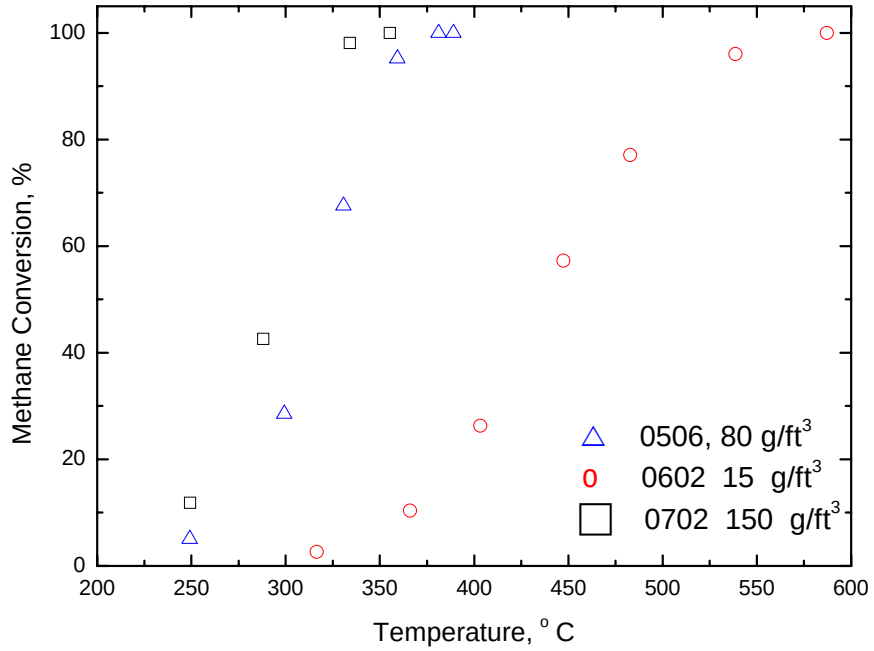

Figure 4.16 Comparison among extinction curves of Pd loadings; Run#: 0506, 0602, 0702; Cat. = Pd wash coat catalysts, 1.20 g, aged and reduced CH_4 = 10% methane in nitrogen, 9.5±0.2 mL/min, 4700±150 ppm; Air = 198±1.5 mL/min

4.2.2 Methane concentration effects

In this part, three methane concentrations, 3100±100, 4700±150 and 8500±300 ppm, were used on Cat. 6 (Pd loading 15 g/ft^3) to investigate the effect of methane concentration on conversion. The results given from Fig. 4.17 to 4.22. Fig. 4.17 to 4.19 are illustrations of individual ignition and extinction curves with different methane concentration. Fig.4.20 and 4.21 show comparisons of the three ignition and extinction curves, and Fig. 4.22 shows the converted methane amount.

The primary result of interest observed in this set of experiments was an increasing ignition temperature as the methane concentration increased. In other words, the ignition and extinction curves shifted to the right and a higher temperature was required to achieve the same conversion. This behaviour is indicative of self-inhibition by methane. Self-inhibition by reactants in catalytic system is common, and, for example, is reflected in Langmuir-Hinshelwood-Hougen-Watson (LHHW) type rate models. Self inhibition is also common in catalytic combustion applications such as the oxidation of CO or C_3H_6 over Pt (Voltz et al., 1973). However, for the catalytic combustion of methane over Pd, the consensus in the literature is that the reaction follows a roughly first order rate in methane concentration, as discussed in Chapter 2. In this case, it would be expected that the ignition curve would shift to the left with increasing methane concentration, because the rate of reaction would increase. This latter behaviour was observed by Hayes et. al (2001). They studied the catalytic combustion of methane over a Pd catalyst over the concentration range of 3900 to 14, 300 ppm.

A possible explanation for methane inhibition is water effects. Because water is known to inhibit the rate, the activities of catalysts will certainly become lower when methane concentration increased due to the fact that more water is

generated (more methane is converted). But it is doubtful that this is the explanation. Hayes et al. (2001) noted that the water produced by the methane combustion caused rate inhibition; however, fractional conversion still increased with increasing methane concentration. Litto (2008) studied the same catalyst used in the present investigation, using the 80 g/ft^3 catalyst in monolith form. He performed kinetic modeling and found that it was necessary to include an inhibition term for methane in his model. It is clear that this catalyst differs significantly from others reported in the literature.

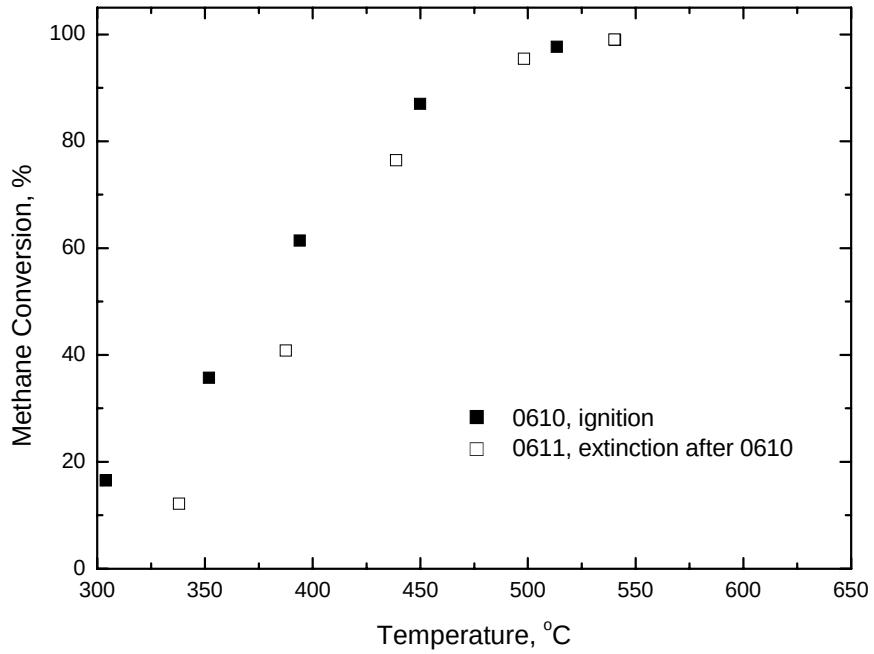

Figure 4.17 Ignition and extinction curves of methane combustion: methane effects; Run#: 0610, 0611; Cat. = Pd wash coat catalysts, 15 g/ft^3, 1.20 g, aged and reduced; CH_4 = 10% methane in nitrogen, 6.2±0.1 mL/min, 3100±100 ppm; Air = 198±1.5 mL/min

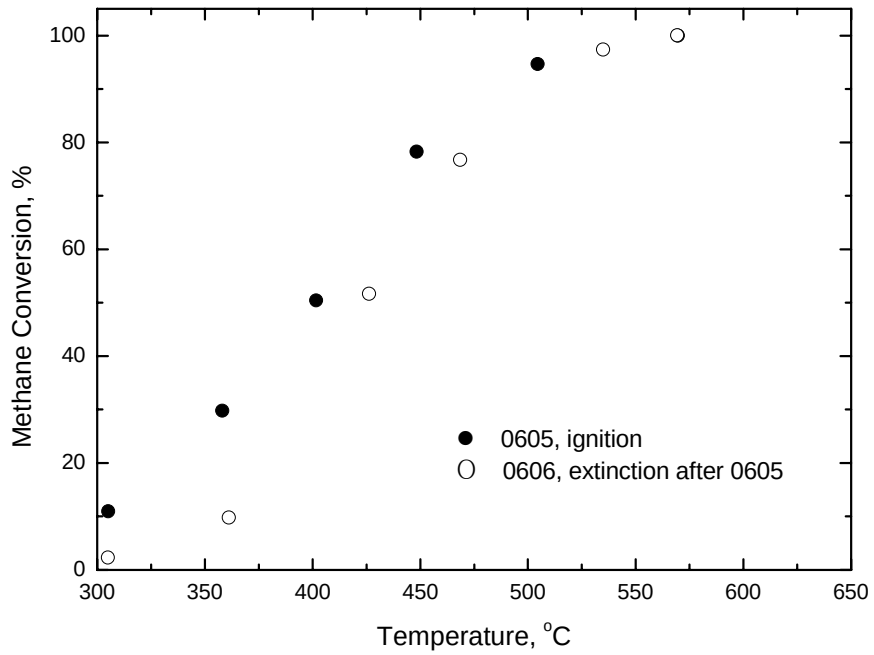

Figure 4.18 Ignition and extinction curves of methane combustion: methane effects; Run#: 0605, 0606; Cat. = Pd wash coat catalysts, 15 g/ft^3, 1.20 g, aged and reduced; CH_4 = 10% methane in nitrogen, 9.5±0.2 mL/min, 4700±150 ppm; Air = 198±1.5 mL/min

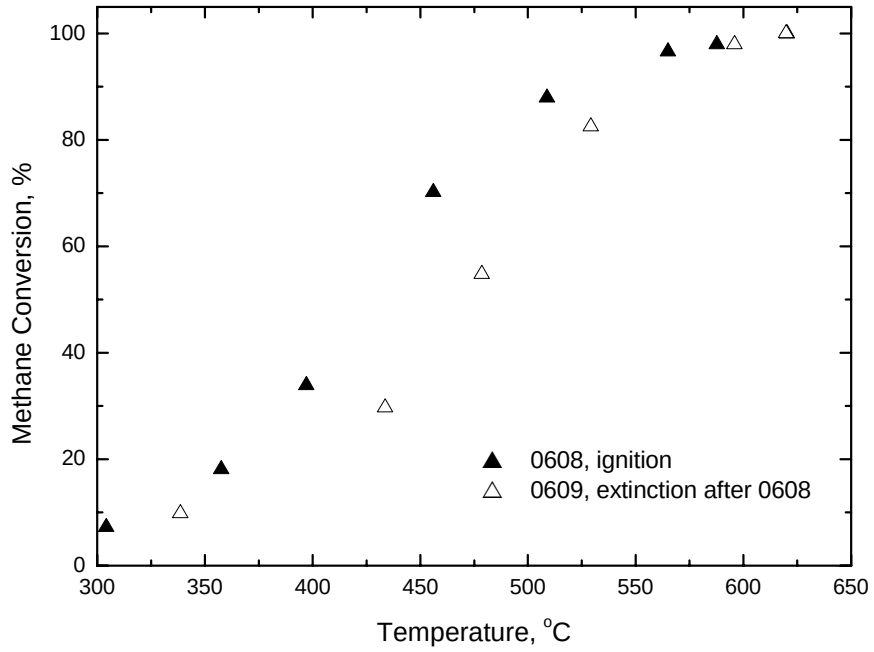

Figure 4.19 Ignition and extinction curves of methane combustion: methane effects ; Run#: 0608, 0609; Cat. = Pd wash coat catalysts, 15 g/ft^3, 1.20 g, aged and reduced; CH_4 = 10% methane in nitrogen, 1.7±0.4 mL/min, 8500±300 ppm; Air = 198±1.5 mL/min

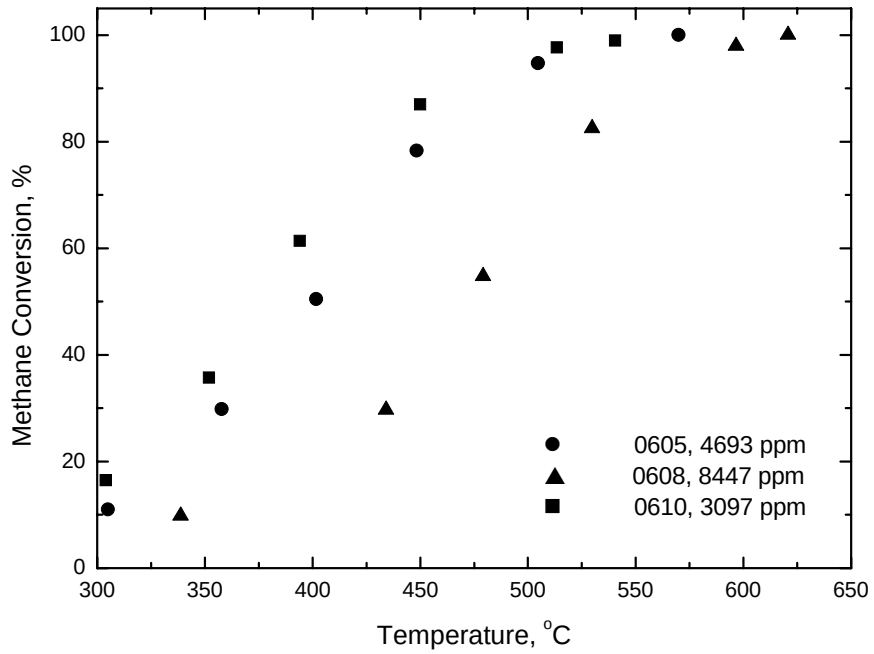

Figure 4.20 Comparison of ignition curves with different methane concentrations; Run#: 0605, 0608. 0610; Cat. = Pd wash coat catalysts, 15 g/ft^3, 1.20 g, aged and reduced; CH_4 = 10% methane in nitrogen, 3100±100, 4700±150, 8500±300 ppm;

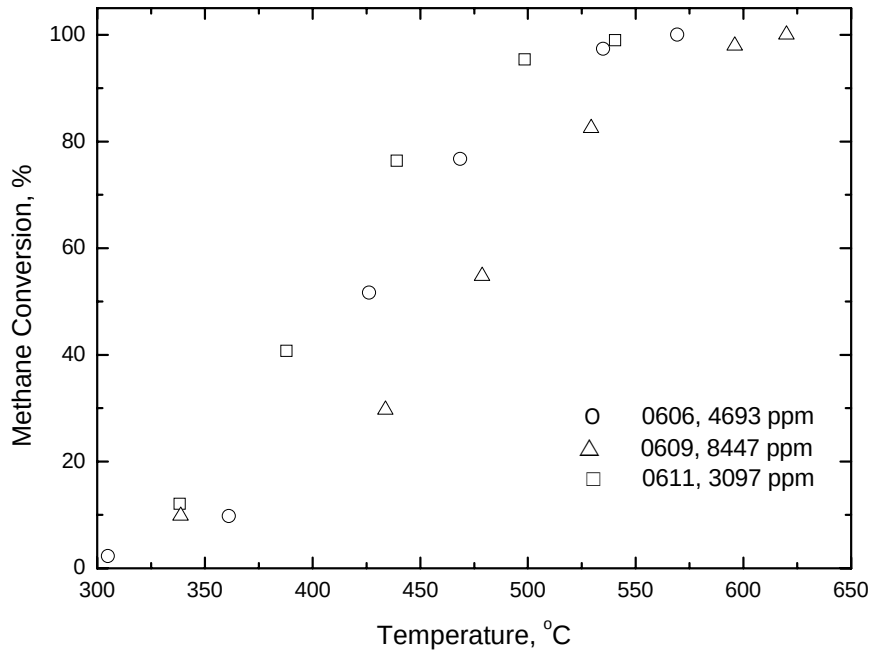

Fig. 4.21 Comparison of extinction curves with different methane concentrations; Run#: 0606, 0609. 0611; Cat. = Pd wash coat catalysts, 15 g/ft^3, 1.20 g, aged and reduced; CH_4 = 10% methane in nitrogen, 3100±100, 4700±150, 8500±300 ppm;

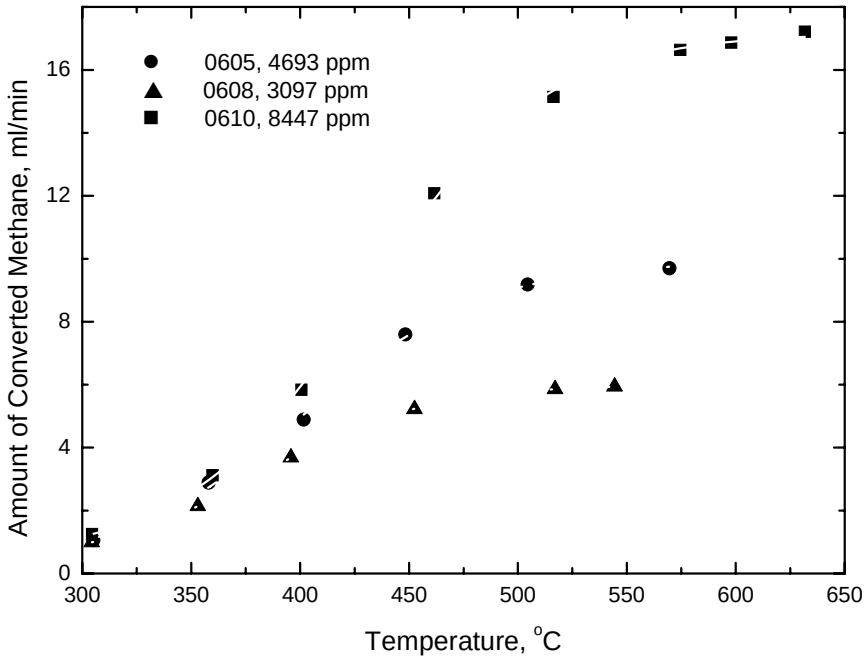

Fig. 4.22 Amount of converted methane at ignition with different methane concentrations; Run#: 0605, 0608. 0610; Cat. = Pd wash coat catalysts, 15 g/ft^3, 1.20 g, aged and reduced; CH_4 = 10% methane in nitrogen, 3100±100, 4700±150, 8500±300 ppm;

4.2.3 The effect of added water

Water is well known to inhibit catalytic combustion reactions, including the Pd catalysed catalytic combustion of methane, as noted in the literature survey in Chapter 2. For example, Hayes et al (2001) showed that the water produced by the combustion was sufficient to effect the catalyst activity, and additional water caused significant further reduction in conversion. Litto (2008), who used one of the types of catalysts employed in the current study, also showed that both water produced by the reaction and added water caused activity loss. If a Pd catalyst is used in automotive exhaust gas after treatment applications, up to 10 % water will be present in the reactor feed. Thus, a series of experiments was performed to elucidate the effect of added water. For these experiments, 5 mol % water was added to the feed using a syringe pump.

Injection of additional water was observed to give a gradually changing catalyst activity. Fig. 4.23 to 4.24 show the ignition-extinction curves obtained for the 150 g/ft^3 Pd catalyst with an inlet concentration of methane of 4700±150 pp. Fig. 4.23 shows the first result obtained over a fresh catalyst which was reduced in hydrogen. After this I-E curve was obtained, the catalyst was again reduced in hydrogen and the ignition-extinction (I-E) curve shown in Fig. 4.24 was obtained. This procedure was followed twice more to give the I-E curves shown in Figs. 4.25 and 4.26 respectively. It was observed that for the first experiment (Fig. 4.23) the catalyst activity was similar to the case without added water (Fig. 4.12), but for subsequent cycles the activity declined and the I-E curves shifted to the right. Following two more cycles of reduction and performing I-E curves (results not shown), two I-E curves were generated without using any hydrogen pretreatment step. These curves are shown in Figs. 4.27 and 4.28. These two sets of results show an apparently stable catalyst activity with almost no hysteresis in the ignition and extinction branches. But this stability of activity disappeared when the temperature was

fixed for a deactivation tests of 25 hours (Fig. 4.29), in which the catalyst sample gradually lost its activities with time exponentially .

Further studies indicated that additional water presence inhibits the reaction by direct harm to the catalysts. Fig. 4.30 and 4.31 are results from experiments done on the same catalyst samples without extra water injection. Obviously, when water was stopped, there was no significant changes on methane conversion. Catalysts were much less active than former no water runs, and extinction stage was even a little more active than ignition stage, completely dissimilar from the observation above. As an effort to recover the catalysts, long time oxidation and reduction were both used (Fig. 4.32, 4.33). The used catalyst samples were heated in air flow at 520°C for 5 hours, and then reduced in hydrogen flow at 570 °C for 5 hours. Unfortunately, the lost activity could not be completely restored, although reduction did make a difference on recovery of catalysts' activity, and their performance did not become the same as before. To sum up, additional water vapour in the feeds may lead to some permanent changes of the catalysts.

Two deactivation tests were also carried out at 585°C for better understanding of water effect (Fig. 4.33 and 4.34). The first procedures of deactivation tests were the same as typical ignition. At the extinction stage, when the temperature reached 585°C, cooling was stopped so the temperature remained constant to deactivate the catalysts. The deactivation curve generally followed traditional catalyst deactivation trend, an exponential decrease. When water was stopped, the conversion rapidly grew from 70% to 90 % within an hour, and kept going for a long time. As a premature speculation, this 20 % conversion might be caused by the reactant inhibition effect from water, while a new surface structure caused by additional water would be responsible for the incomplete conversion of methane at a temperature 200 °C higher than the complete conversion temperature of a new catalyst sample.

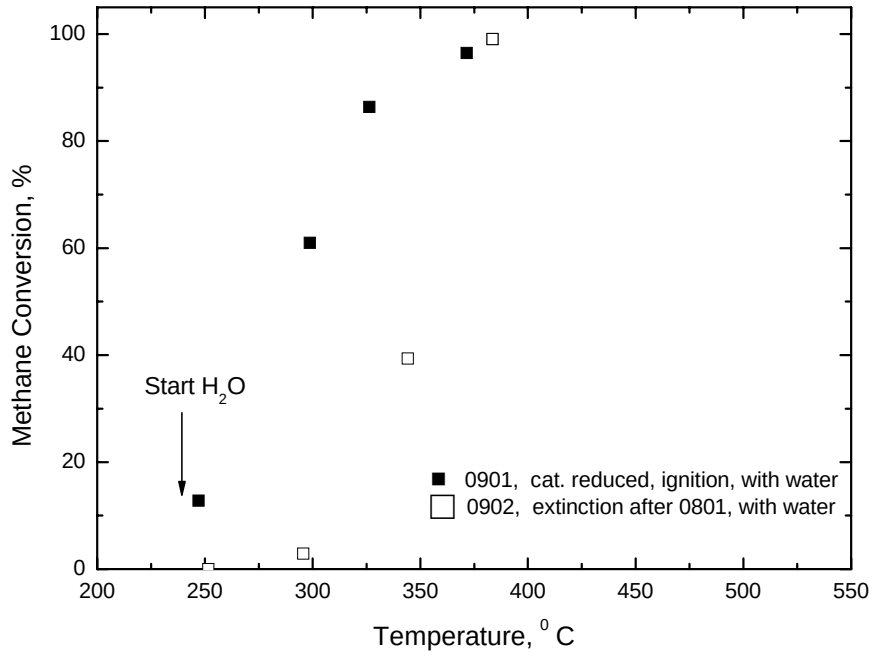

Figure 4.23 Ignition and extinction curves of methane combustion: water effects; Run#: 0901, 0902; Cat. = Pd wash coat catalysts, 150 g/ft^3, 1.20 g (fresh catalysts, reduced)CH_4 = 10% methane in nitrogen, 9.5±0.2 mL/min, 4700±150 ppm; Air = 198±1.5 mL/min; H_2O=0.5 mL/h

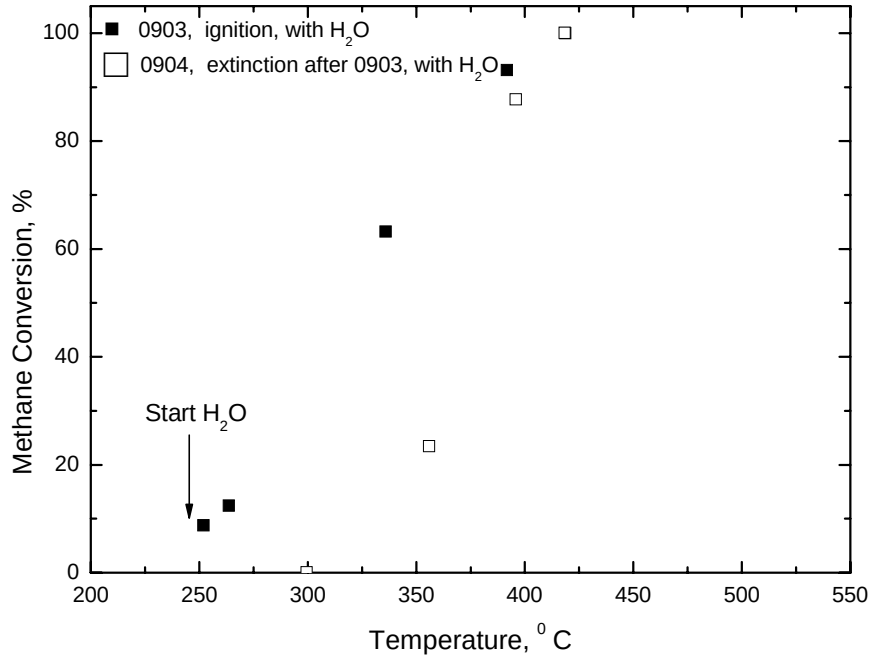

Figure 4.24 Ignition and extinction curves of methane combustion: water effects; Run#: 0903, 0904; Cat. = Pd wash coat catalysts, 150 g/ft^3, 1.20 g (used catalysts, reduced); CH_4 = 10% methane in nitrogen, 9.5±0.2 mL/min, 4700±150 ppm; Air = 198±1.5 mL/min; H_2O=0.5 mL/h

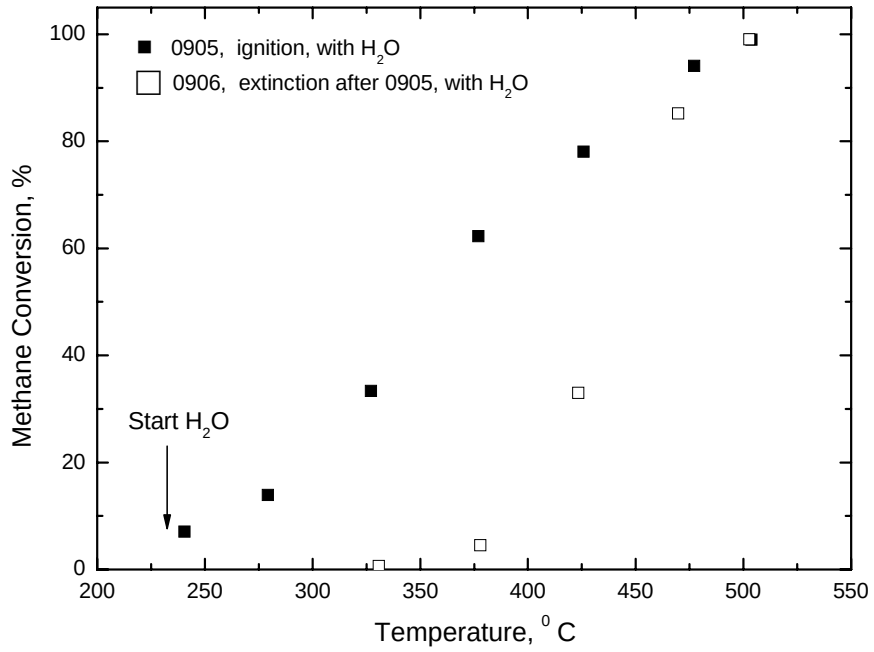

Figure 4.25 Ignition and extinction curves of methane combustion: water effects; Run#: 0905, 0906; Cat. = Pd wash coat catalysts, 150 g/ft^3, 1.20 g (used catalysts, reduced); CH_4 = 10% methane in nitrogen, 9.5±0.2 mL/min, 4700±150 ppm; Air = 198±1.5 mL/min; H_2O=0.5 mL/h

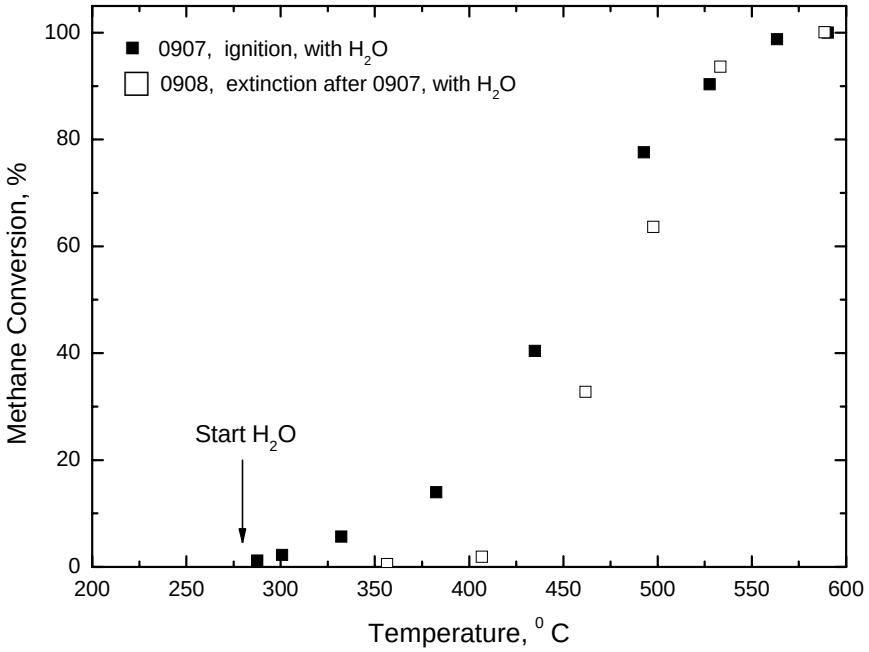

Figure 4.26 Ignition and extinction curves of methane combustion: water effects; Run#: 0907, 0908; Cat. = Pd wash coat catalysts, 150 g/ft^3, 1.20 g (used catalysts, reduced); CH_4 = 10% methane in nitrogen, 9.5±0.2 mL/min, 4700±150 ppm; Air = 198±1.5 mL/min; H_2O=0.5 mL/h

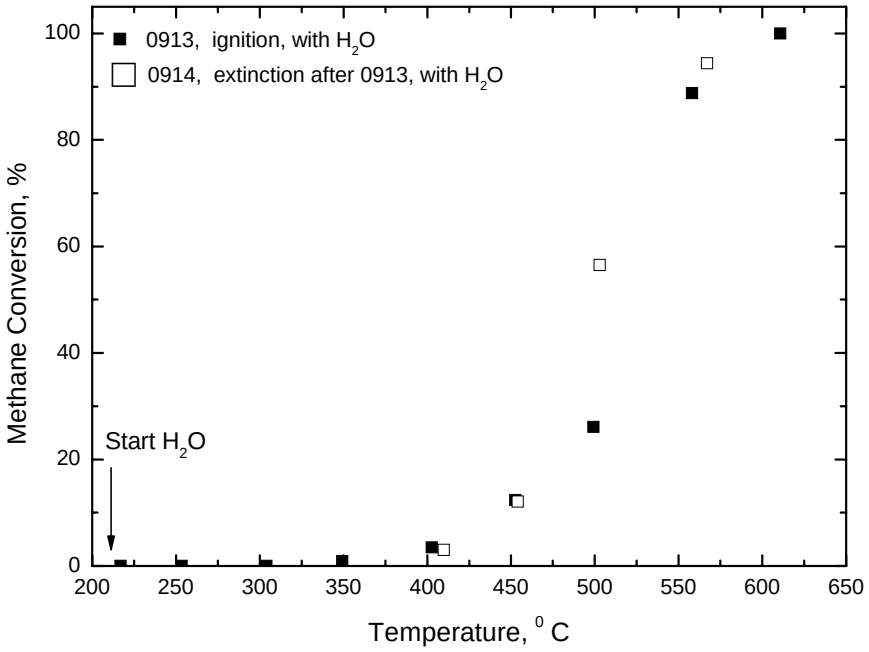

Figure 4.27 Ignition and extinction curves of methane combustion: water effects; Run#: 0913, 0914; Cat. = Pd wash coat catalysts, 150 g/ft^3, 1.20 g (used catalysts); CH_4 = 10% methane in nitrogen, 9.5±0.2 mL/min, 4700±150 ppm; Air = 198±1.5 mL/min; H_2O=0.5 mL/h

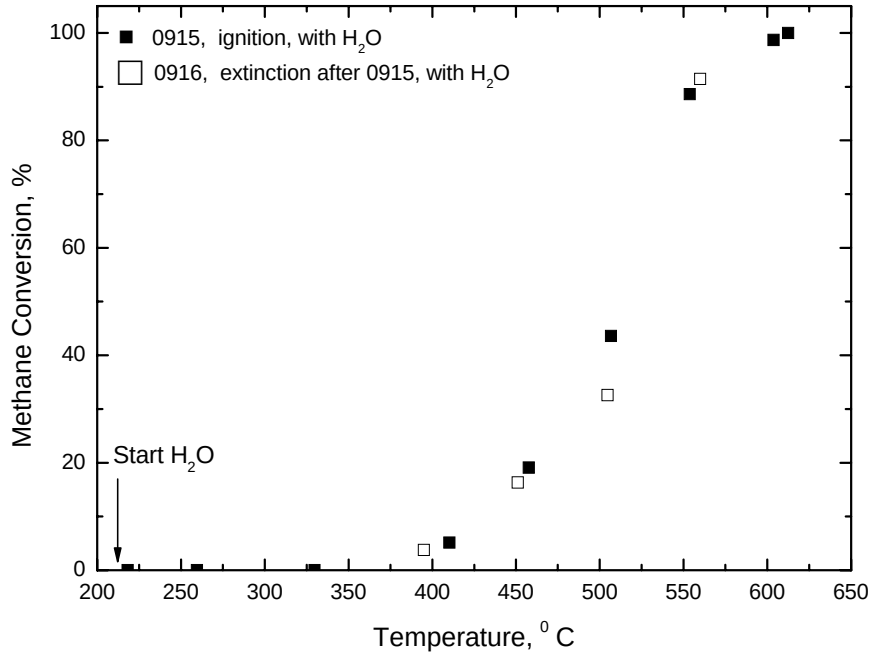

Figure 4.28 Ignition and extinction curves of methane combustion: water effects; Run#: 0915, 0916; Cat. = Pd wash coat catalysts, 150 g/ft^3, 1.20 g (used catalysts); CH_4 = 10% methane in nitrogen, 9.5±0.2 mL/min, 4700±150 ppm; Air = 198±1.5 mL/min; H_2O=0.5 mL/h

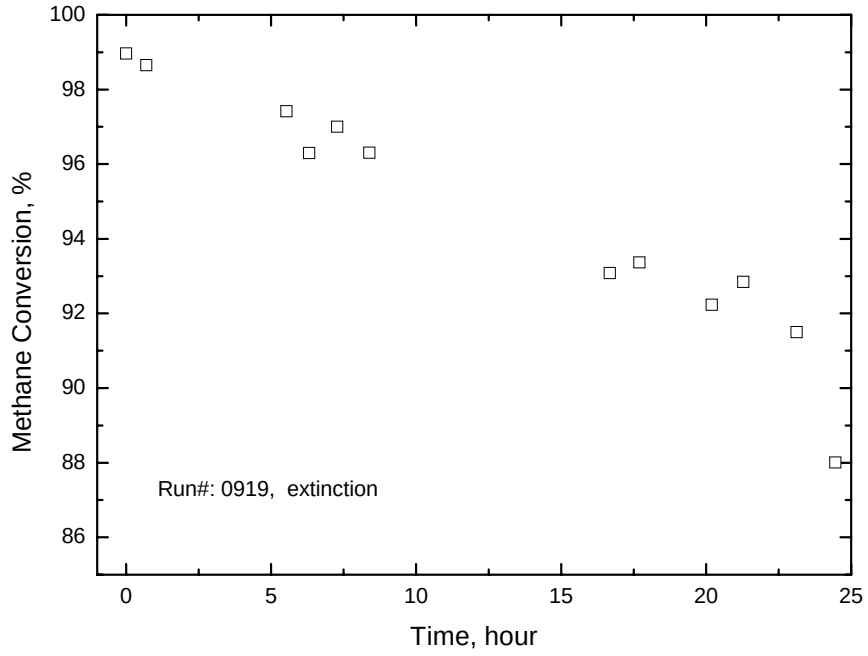

Figure 4.29 Deactivation Test with additional water; Run#: 0919, deactivation; Cat. = Pd wash coat catalysts, 150 g/ft^3, 1.20g (used catalysts); CH_4 = 10% methane in nitrogen, 9.5±0.2 mL/min, 4700±150 ppm; Air = 198±1.5 mL/min; H_2O=0.5 mL/h

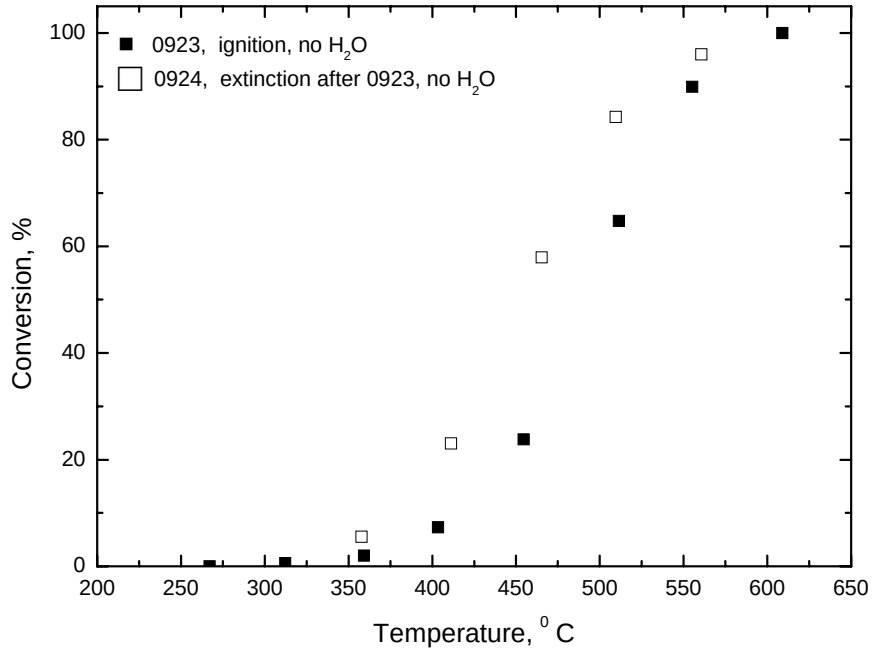

Figure 4.30 Ignition and extinction curves of methane combustion: water effects; Run#: 0923, 0924; Cat. = Pd wash coat catalysts, 150 g/ft^3, 1.20 g (used catalysts); CH_4 = 10% methane in nitrogen, 9.5±0.2 mL/min, 4700±150 ppm; Air = 198±1.5 mL/min; no H_2O

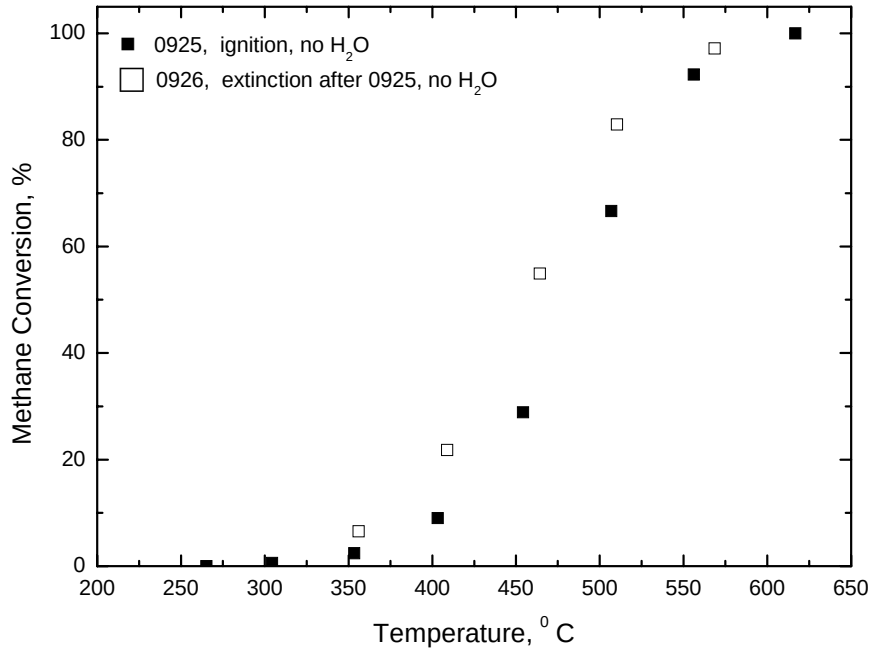

Figure 4.31 Ignition and extinction curves of methane combustion: water effects; Run#: 0925, 0926; Cat. = Pd wash coat catalysts, 150 g/ft^3, 1.20 g (used catalysts); CH_4 = 10% methane in nitrogen, 9.5±0.2 mL/min, 4700±150 ppm; Air = 198±1.5 mL/min; no H_2O

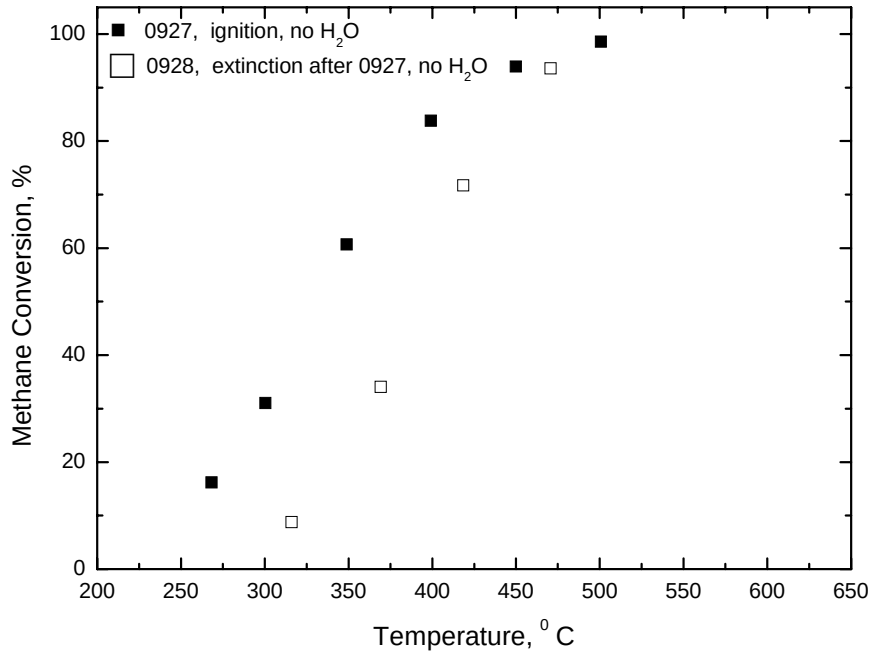

Figure 4.32 Ignition and extinction curves of methane combustion: water effects; Run#: 0927, 0928; Cat. = Pd wash coat catalysts, 150 g/ft^3, 1.20 g (used catalysts, reduced); CH_4 = 10% methane in nitrogen, 9.5±0.2 mL/min, 4700±150 ppm; Air = 198±1.5 mL/min; no H_2O

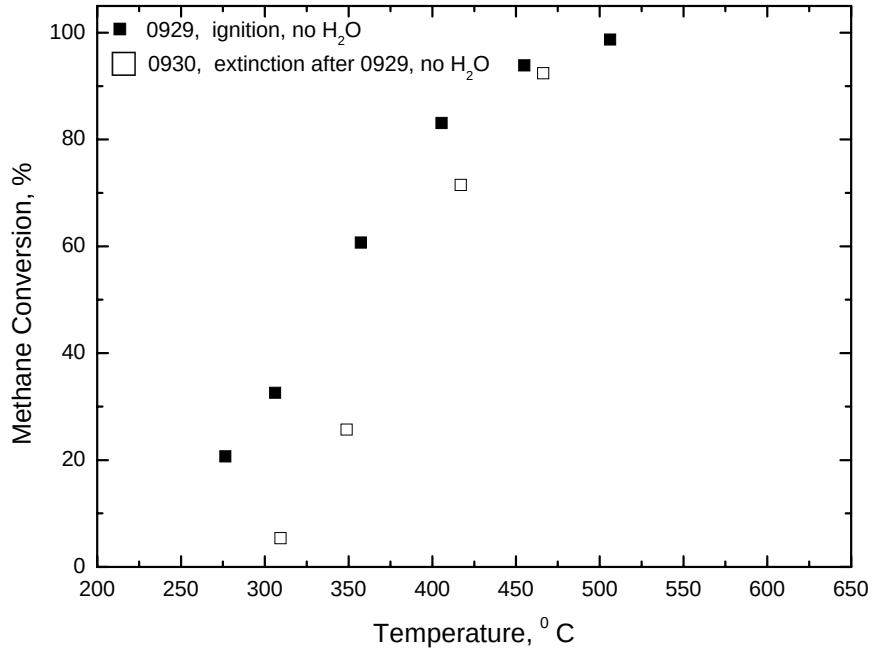

Figure 4.33 Ignition and extinction curves of methane combustion: water effects; Run#: 0929, 0930; Cat. = Pd wash coat catalysts, 150 g/ft^3, 1.20 g (used catalysts, reduced); CH_4 = 10% methane in nitrogen, 9.5±0.2 mL/min, 4700±150 ppm; Air = 198±1.5 mL/min; no H_2O

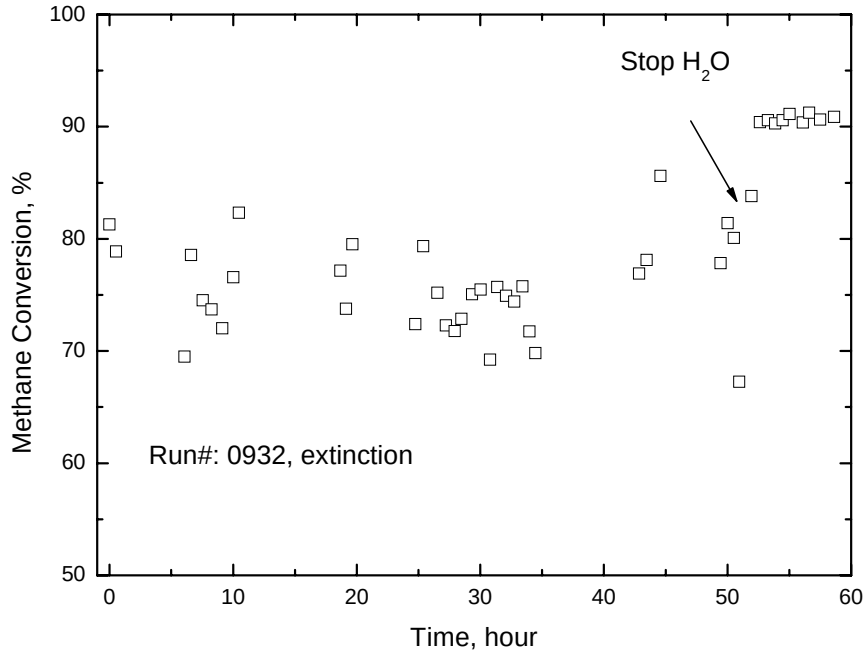

Figure 4.34 Deactivation test with additional water and then cutting off Run#: 0932, deactivation; Cat. = Pd wash coat catalysts, 150 g/ft^3, 1.20 g (used catalysts); CH_4 = 10% methane in nitrogen, 9.50mL/min, 4700±150 ppm; Air = 198±1.5 mL/min; H_2O=0.5 mL/h

4.3 Methane combustion on different Pd states

4.3.1 The performance of catalysts at high temperature

Fig. 4.35 shows the behavior of Cat. 4 at high temperature. The sample was heated in nitrogen flow at 870℃ for 2.5 hours, then cooled down to 800℃ and methane flow was started to test its conversion. A slight decrease and recovery of conversion was seen on the curve within the region of 650-775℃. Same situation has been reported by other investigators (e.g. Lyubovsky and Pfefferle 1998, Gelin et al., 2002), although the decrease and recovery of activity in this work is much less drastic. An explanation for this phenomenon is that the phase transformation of PdO to Pd takes place at above 800℃. In air at 1 bar pressure, PdO decomposes to Pd, which has been observed to be the less active phase for methane oxidation. Therefore, in the beginning of the extinction curve, Pd is the active phase. However, the Pd begins to be oxidized back to PdO at about 800℃, and thence the activity recovers with the phase transformation to 100 %.

4.3.2 The influence of reduction and oxidation

Many studies in the literatures have reported experiment results regarding to the activity of Pd phase and PdO phase, and a conclusion has been reached that PdO will transform to Pd with the presence of oxygen at temperature higher than 1100K. It is quite controversial, however, when it comes to whether Pd or PdO is more active. Moreover, as implied above, water might lead to a new surface structure or phase on the catalysts, so it is necessary to analyze the reaction of methane combustion on different catalyst phases to find out which one of them has the best activity. No extra water feed is involved in this section. The testing results on three catalysts with different Pd loadings are shown in Fig. 4.36 (150 g/ft^3), Fig. 437 (80 g/ft^3) and Fig. 4.38

(15 g/ft^3). Three states were involved in these experiments: the reduced state, the oxidized state and the after-ignition state. They are produced through the following procedures:

First, the reduced state: the temperature of the reactor was first raised to 370℃, at which H_2 flow was started. Then the temperature was increased to 570℃ to reduce the catalysts. This step took 15 minutes. After that the H_2 flow was cut off.

Second, the oxidized state:. the catalyst sample was first reduced as above; then the temperature in the reactor was set to 520℃ and kept stable. When reactor temperature reached this stage, air flow was started. Catalysts would be heated under this condition for 5 hours.

The activities of these two states were investigated by a cooling test (extinction). Temperature of the reactor was first fixed to a level that all the methane could be converted, and the temperature was decreased by 50℃ increments step by step while the conversion was tested at every step. The results were compared with the third state, after-ignition state, which was presented by the methane conversion from extinction branches of ignition-extinction tests. It is obvious from three figures that reduced states were always the most active, whilst after-ignition states were the least. Considering this with the aforementioned results, one will have a better understanding about the roles of reduction and water on these catalysts. More interesting is, the performance of oxidized states seemed to vary from as lowly active as after ignition states, to as highly active as reduced phases, depending on the Pd loadings of the catalysts. If oxidation time changed (Fig. 4. 39) from one hour to two hours to five hours, there was no huge difference between the three curves, but the catalysts with shortest oxidizing time seemed to be a little more active than the other two.

Till now there seem to be two contradictory discoveries about catalyst states and their activities. From the above discussions (Fig. 4.36 to 4.39), as well as earlier analysis about the effects of reduction and ageing (Fig. 4.8 and 4.9), it can be concluded that reduced catalysts usually were, although not always apparent, more active than oxidized catalysts. But as confirmed by the catalysts' behaviour at high temperature (Fig 4.35), Pd is less active than PdO. This inconsistence can be explained as follows. First of all, many researchers have reported the significant loss and recovery of catalyst activities at around 800℃, which was attributed to the phase transformation of Pd to PdO, and based on this fact they implied that PdO was more active than Pd. In this work, the loss and recovery of activities at around 800℃ did exist, but in a very small scale. Hence it can be concluded that in these catalysts, the activities of Pd and PdO are not quite different. Secondly, judging from the XRD analysis (discussed later), the possibility cannot be ruled out that there is still some traces of PdO on the catalysts after the reducing pretreatment. According to Zheng and Altman (2000), partially reduced catalysts, or a mixture of Pd and PdO sometimes have the most activity.

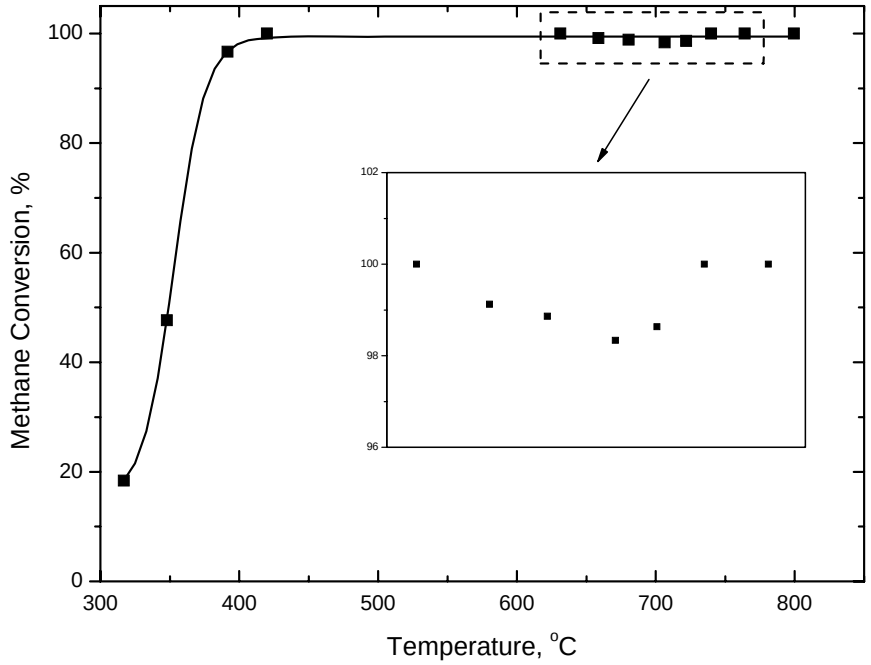

Figure 4.35 The high temperature extinction curve for methane combustion ; Run#: 0430; Cat. = Pd wash coat catalysts, 150 g/ft^3, <1.20 g CH_4 = 10% methane in nitrogen, 9.50mL/min, 4700±150 ppm; Air = 198±1.5 mL/min;

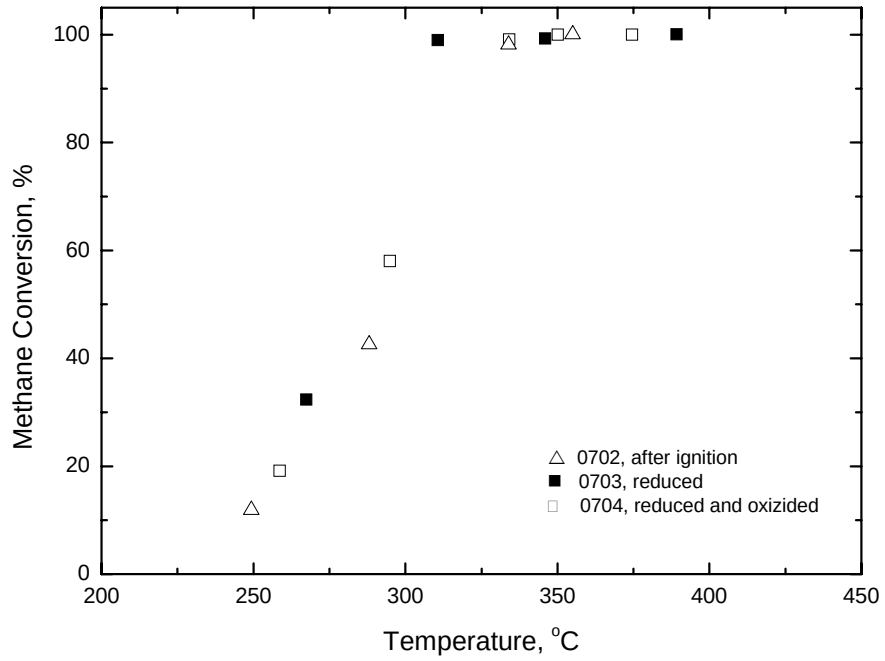

Figure 4.36 Comparison among extinction branches of different states Run#: 0702, 0703, 0704; Cat. = Pd wash coat catalysts, 150 g/ft^3, 1.20 g CH_4 = 10% methane in nitrogen, 9.5±0.2 mL/min, 4700±150 ppm; Air = 198±1.5 mL/min;

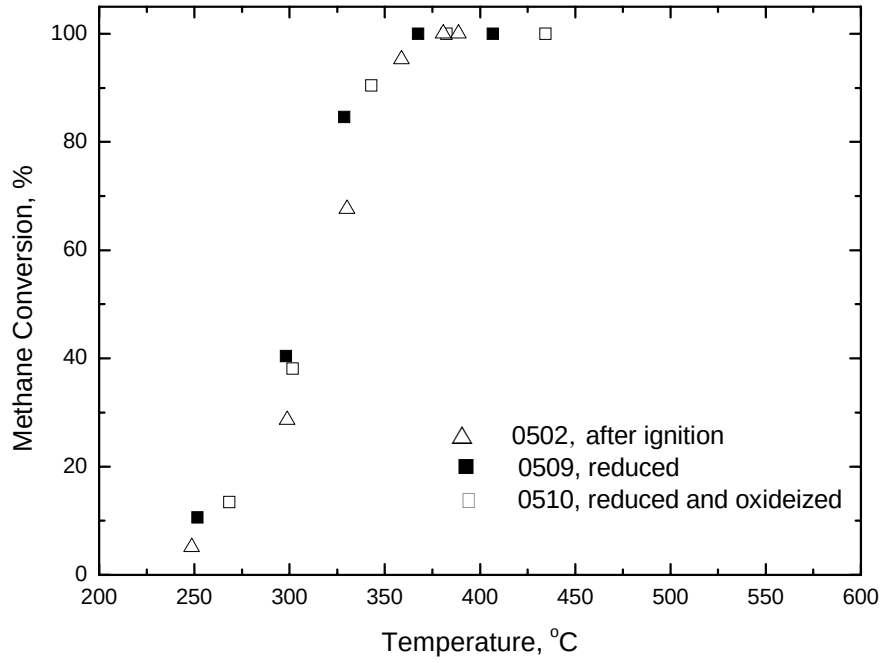

Figure 4.37 Comparison among extinction branches of different states Run#: 0502, 0509, 0510; Cat. = Pd wash coat catalysts, 80 g/ft^3, 1.20 g CH_4 = 10% methane in nitrogen, 9.50mL/min, 4700±150 ppm; Air = 198±1.5 mL/min;

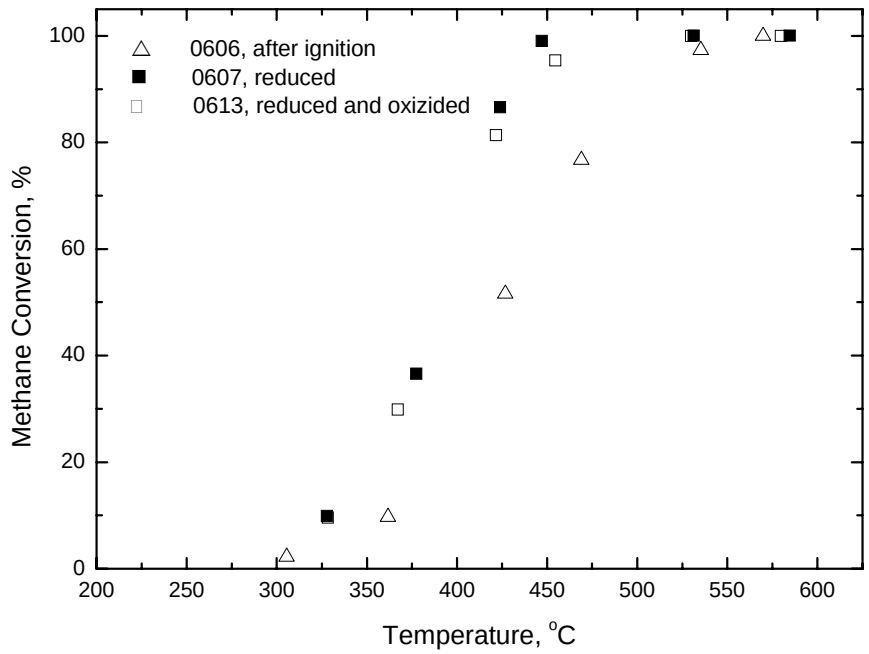

Figure 4.38 Comparison among extinction branches of different states Run#: 0606, 0607, 0613; Cat. = Pd wash coat catalysts, 15 g/ft^3, 1.20 g CH_4 = 10% methane in nitrogen, 9.50mL/min, 4700±150 ppm; Air = 198±1.5 mL/min;

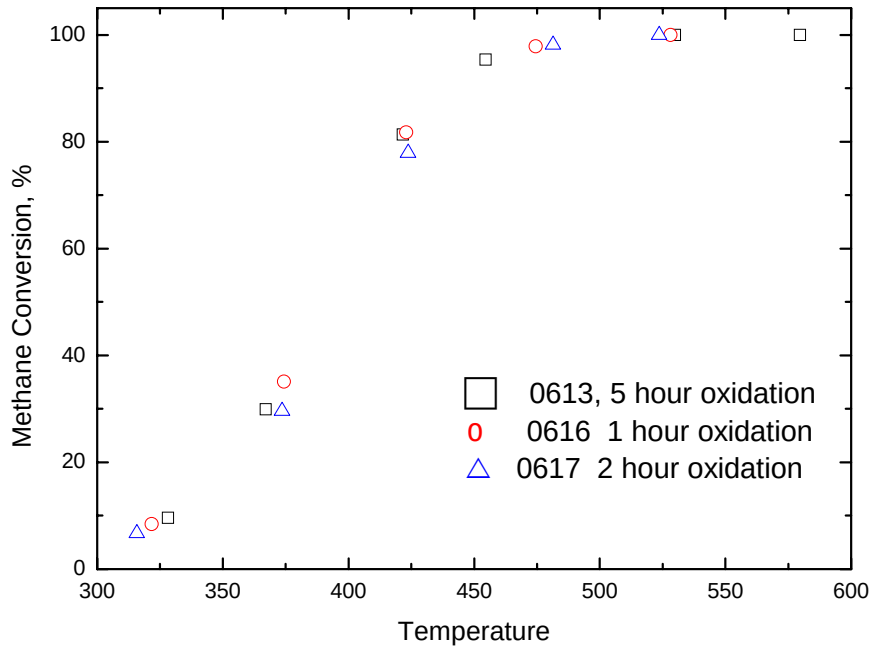

Figure 4.39 Comparison among extinction branches with varied oxidizing times

Run#: 0613, 0616, 0617; Cat. = Pd wash coat catalysts, 15 g/ft^3, 1.20 g

CH_4 = 10% methane in nitrogen, 9.50mL/min, 4700±150 ppm; Air = 198±1.5 mL/min;

4.4 Characterization of catalysts and analysis

4.4.1 Instrumental Neutron Activation Analysis (INAA)

Although the three different catalysts were labeled with Pd loadings of gram per cubic feet by the manufacturer, it is still worthwhile to determine the mass fraction of Pd on these catalysts for better comparisons with other catalysts in the literature. Meanwhile, beside Pd and Al_2O_3, these catalysts may contain some other components which are in low amount but probably have significant contribution to the unique performance of the catalysts. Answers towards these two questions would be available with the help of INAA.

Table 4.2 show the results if the INAA analyses. Notice that the samples used were mixtures of washcoats as well as substrates. The first important information in this table are the mass fractions of Pd in the three types of catalysts: about 0.42 % for the catalysts with 150 g/ft^3 Pd, 0.31% for those with 80 g/ft^3 and 0.46% for those with 15 g/ft^3. Recall the estimation of Pd concentrations of three catalysts. The ten times difference in magnitude is because the samples in INAA contained washcoats. INAA results partially explain why these catalysts have outstanding abilities of methane conversion because they contain a considerable amount of Pd, especially the one with 150 g/ft^3 Pd loadings. Interestingly, a simple calculation based on these mass fractions reveals that the manufacturer's label on catalysts with 80 g/ft^3 Pd loadings looks to be conflict with the labels from Umicore, as the ratio of the real Pd masses of the three catalysts by NAA is approximately 9.2: 6.7: 1, different from the ratio of 10: 5.3: 1 according to the labels.

Other than Pd, lanthanum (La), one of the important rare earth materials, was detected in these catalysts, and their amount is not proportional to that of Pd. As discussed in Chapter 2, rare earth addictives could improve the activity of

catalysts, which may be another contribution to the high activity of theses catalysts.

Table 4.2 Instrumental Neutron Activation Analysis results

Sample ID	Catalysts (g/ft^3)	Pd (g/g)	± 1σ	La (g/g)	± 1σ
40	150	4240	40	2460	20
41	80	2990	40	3300	40
42	15	454	16	2620	20
43	80	3260	40	3710	40
44	150	4170	80	2420	40
45	15	465	13	3050	20
uncertainty ± 1σ 68% confidence limit					
all concentrations in g/g (ppm)					

4.4.2 X-Ray Diffraction (XRD)

Earlier in this chapter, it was suggested that different pretreatments on the catalysts may lead to different Pd phases, which further cause different behaviours on methane conversion. XRD could provide information on the Pd phases, as well as provide other information such as the grain size and the dispersion of catalyst particles.

Fig. 4.40 shows the XRD patterns for the three catalyst samples obtained from grinding parts of the monolith and washcoat. This was the type sample used in the reaction measurements. The most intense peak for PdO, the 101 line, occurs at 33.8 °2θ, and the most intense peak for Pd, the 111 line, occurs at 40.1 °2θ. No distinct peaks due to Pd and PdO can be seen in Fig. 4.40; the locations of the high intensity lines for PD and PdO are marked in Fig. 4.40.

The sharp lines in the patterns shown in Fig. 4.40 are all due to the monolith support (vide infra). The detectibility of Pd by XRD depends on the Pd concentration and the size of the Pd and/or PdO crystals. Samples with increased Pd concentration were prepared by scrapping the washcoat off the monolith.

XRD patterns of the concentrated Pd samples are shown in Fig. 4.41. The sharp peaks, due to the monolith, are absent from the pattern in Fig. 4.41 The untreated sample has two peaks at about 24 and 34 °2θ; these peaks disappear when the sample is treated at high temperatures during reduction or oxidation. The peaks may be due to some hydrated species present in the Pd support. The oxidized and reduced samples is dominated by the lines due to the support; however, differences in diffraction intensity are noticeable in the regions of the most intense Pd and PdO lines. These differences in intensity are more noticeable in the expanded semi-log plot shown in Fig. 4.42. The differences in reduced and oxidized patterns are easily seem at the location of the most intense PdO line at 33.8 °2θ and the most intense Pd line at 40.1 °2θ.

An even better way of showing the differences in the intensities is to subtract the intensities for the oxidized pattern from the intensities of the reduced pattern. The resulting difference pattern is shown in Fig. 4.43. The difference pattern clearly shows two peaks; one at the PdO 101 line (33.8 °2θ) and one at the Pd 111 line (40.1 °2θ). A less defined peak is present at the Pd 200 line (46.7 °2θ). The full widths at half height (FWHH) of the PdO 101 and the Pd 111 line can be used to estimate the size of the PdO and Pd crystals. The Scherer equations is used for estimation of the crystal size from FWHH (Cullity, 1956). i.e.

$$\mathbf{d_{avg}} = \frac{\mathbf{0.9\lambda}}{\mathbf{(FWHH)\cos(\theta)}} \qquad (4.\ 1)$$

Where d_{avg} is the average crystal diameter, λ is the wave length of the CuKα radiation (= 0.1543 nm); FWHH is the width at half height of the diffracted peak of the species of interest (the subtracted peak) in radians and θ is half of the diffraction angle (16.9 ° for PdO 101 line and 20.05 ° for the Pd 111 line). The FWHH for the PdO 111 line is about 3 ° (0.0524 radians) and about 5 ° (0.0873 radian) for the Pd 111 line. These FWHH values yield, according to the Scherrer equation, average PdO and Pd crystal sizes of 2.8 and 1.7 nm. These sizes are quite approximate since limit of XRD line broadening is in the 1.5 to 2.5 nm range. These results clearly show that the Pd is present as very small crystals; i.e. the Pd is very well dispersed. High dispersion mean a high Pd surface area which usually implies high activity.

The XRD patterns shown in Fig. 4.40 to 4.43 are fairly noisy. The signal to noise ration can be improved by increasing the time per step. One experiment with the concentrated reduced catalysts was done with a 40 s time per step. In Fig. 4.44 the results from this experiment are compared to the experiment done on the same sample with a 4 s time per step. The results show a large decrease in the noise for the 40 s per step run compared to the 4 s per step run. However, the average diffraction intensity of the two runs is essentially the same. This result increases the confidence in the size estimates obtained for the subtraction of two rather noisy patterns. Not all runs were done at step times of 40 s because one scan for 20 to 60 °2θ at 0.05 °2θ and 40 s per step takes about 10 hours.

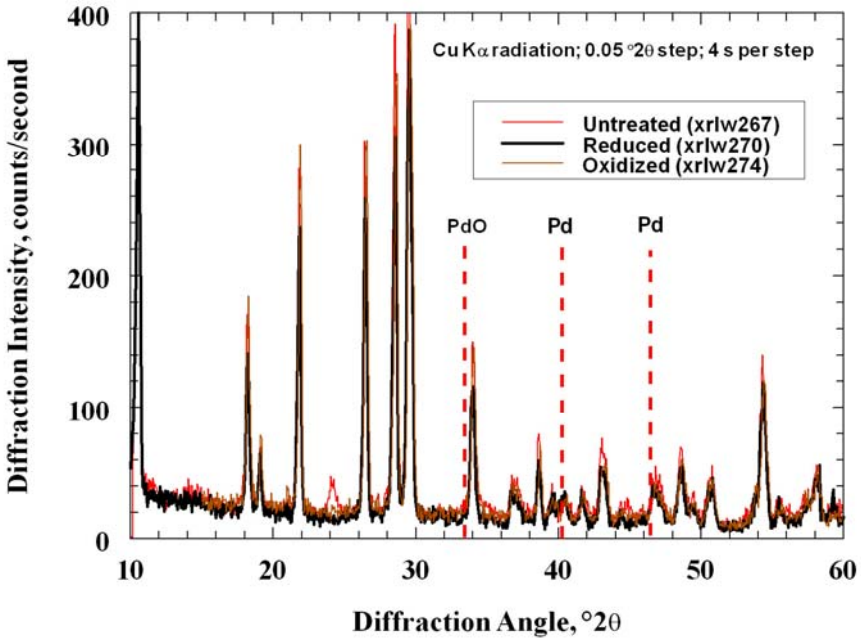

Figure 4.40 XRD patterns for untreated, reduced and oxidized samples (Catalyst: Pd loading = 150 g/ft^3; numbers in parenthesis identify the XRD experiment number).

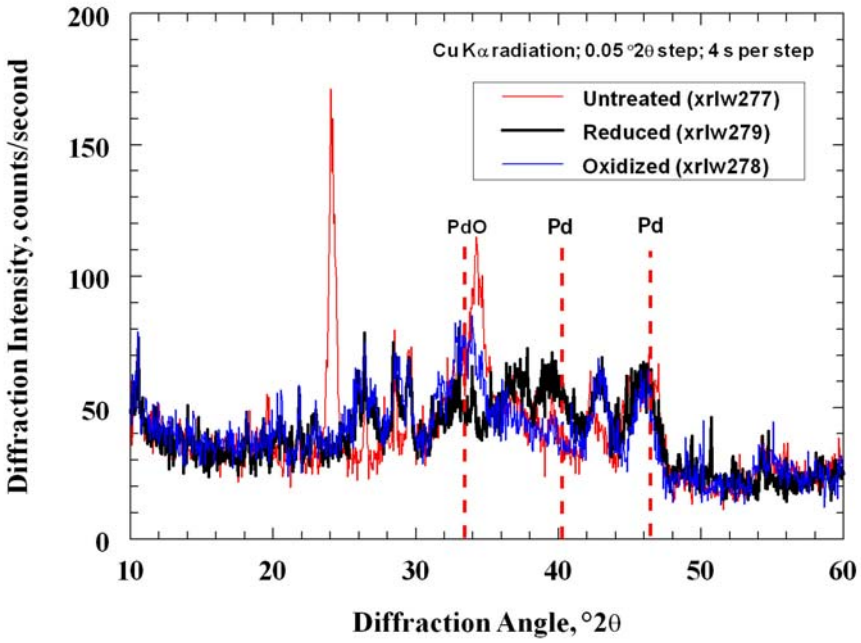

Figure 4.41. XRD patterns for concentrated Pd samples: Untreated, reduced and oxidized. (Samples made from catalyst with a Pd loading of 150 g/ft^3; numbers in parenthesis identify the XRD experiment number).

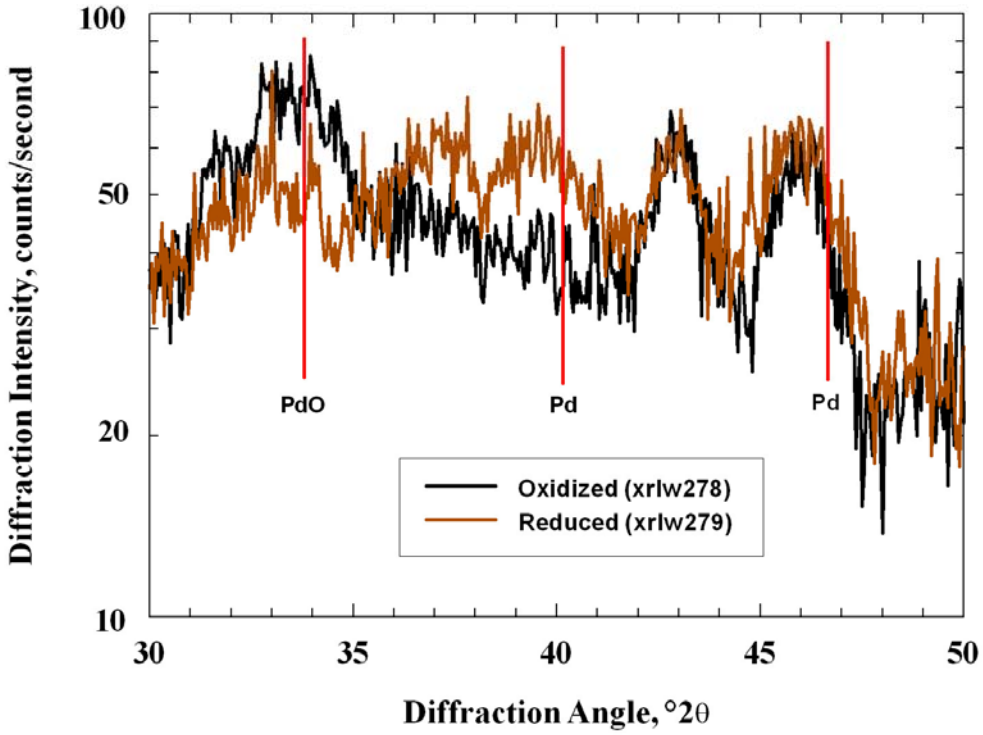

Figure 4.42. Expanded XRD patterns for plots shown in Figure 4.41 of concentrated Pd samples: Reduced and oxidized. (Samples made from catalyst with a Pd loading of 150 g/ft^3; numbers in parenthesis identify the XRD experiment number).

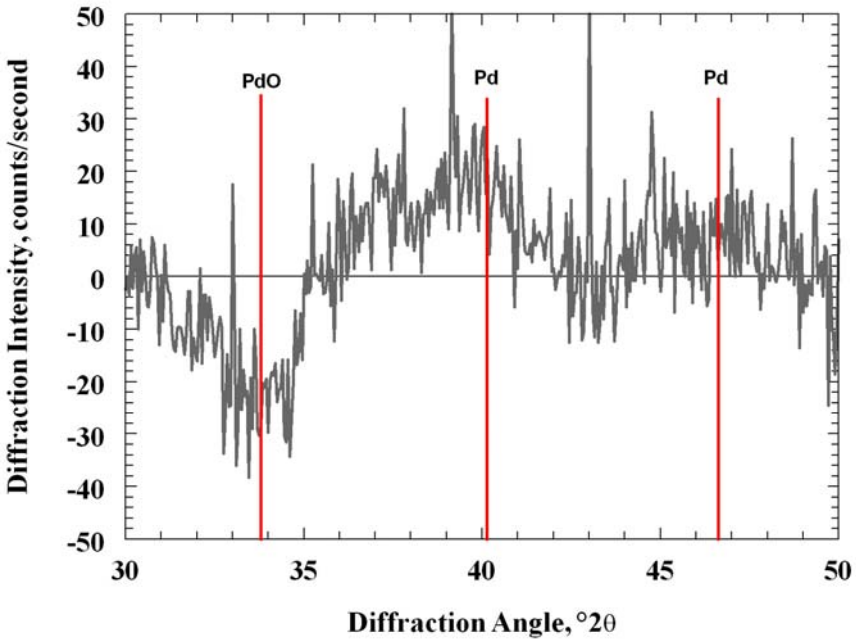

Figure 4.43. Difference XRD pattern obtained by subtraction of the oxidized pattern in Figure 4.42 form the reduced pattern in Figure 4.42.

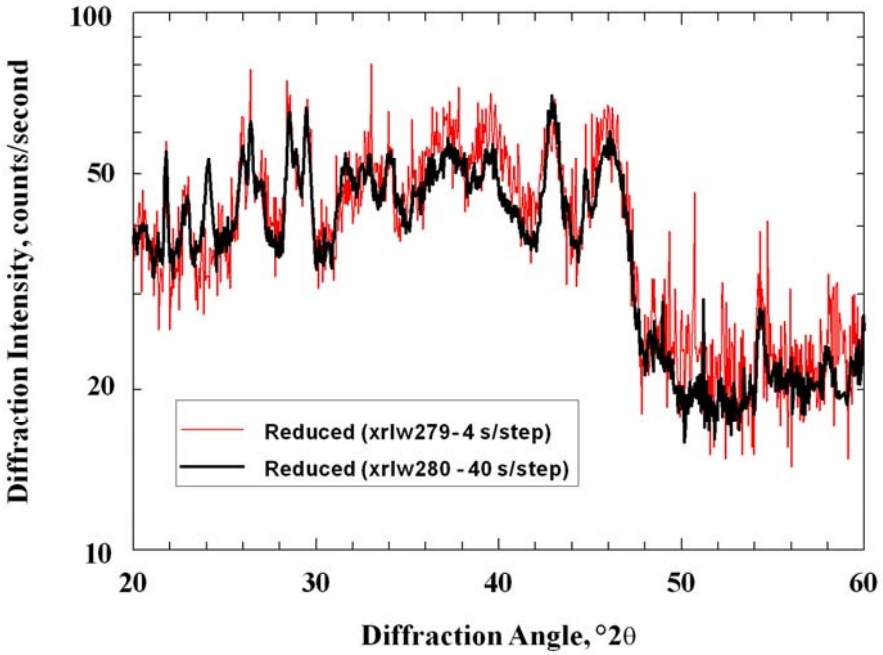

Figure 4.44. Effect of increased counting time per step on XRD patterns for reduced concentrated sample

Chapter 5 Summary and Future Work

5.1 Summary

5.1.1 General behaviours of the catalysts

Several phenomena were observed from the patterns of ignition and extinction of the catalyst samples. First, catalysts have decent methane oxidation abilities at relatively low temperature. Tests on the heavily-loaded samples with 150 and 80 g/ft^3 Pd showed that all the methane was converted below 400 ^{o}C. What is more, the conversion of methane at ignition branches, especially on lightest loaded catalysts with 15 g/ft^3 Pd were usually higher than that of extinction stages, contradicting to the former consensus know as “hysteresis”. Combined with the later discovery of water effects, his unconventional performance could be attributed to the harm of water. But also, this phenomenon may be related to the temperature distribution inside of the reactor since the temperature used in analysis was from down stream,

5.1.2 Influence of various pretreatments

Three pretreatments were used in this project. Reduction could highly improve the catalyst’s activity as well as stabilize its performance, making the results under the same condition consistent (without water). Ageinng also had some enhancing effects on the catalyst’s performance, but not significantly. The catalysts after oxidation became a little less active than the reduced samples.

5.1.3 Influence of methane concentration

Different from most literatures, in this work methane had important inhibition on the reaction. With the increase of methane concentration, the conversion of

methane at the same temperature decreased, despite that the increase of converted amount. According to the simulation of a former researcher (Litto 2008), it is not the result of additional water generated by extra methane. Methane inhibition is highly possible to be a unique finding on these catalysts due to their compositions.

5.1.4 Influence of addition of water in the feeds

The performance of catalysts was completely different with former runs without extra water. First of all, with the presence of water in the feeds, reduction could not lead to reproducible results among tests with same reaction conditions. Secondly, catalysts lost a large amount of activity after tests with water. Finally and most importantly, when the addition of water was stopped, the lost activity still could not recover fully, even with the help of reduction, which resulted in the assumption that a new surface state of catalysts was generated by water. To sum up, water has a strong negative influence on the catalysts.

5.1.5 Preliminary characterization

Instrumental neutron activation analysis (INAA) and X-ray diffraction (XRD) were done on the catalyst samples. From the results of INAA, the real Pd concentrations (on both washcoats and substrates) were obtained along with the fact that catalysts contain some Lanthanum (La), possibly as addictives. From the results of XRD, it was found that most of the palladium on reduced catalysts existed in the form of PdO, while oxidized catalysts had more Pd. It was also inferred that the catalytic particles were dispersed very well on the supports.

5.2 Future Work

5.2.1 Gas constituents

The gas feeds involved in this project are much simpler than real exhaust gases from natural gas turbines, which contain not only methane and water, but also much carbon dioxide, some carbon monoxide, and trivial oxides of nitrogen, according to many former research such as Fino et al., (2007). The behavior of the catalysts will be a lot different under this complex gas atmosphere. First of all, a number of gas components may inhibit the reaction, although some scholars argued differently (Salaun et al., 2009). Secondly, the catalysts should be also capable of degrading NO_x and CO. Finally, the real exhausted gas will contain water with mole fraction much higher than what used in this experiment, believed to be at least 10 %. Additional hydrogen in gas feeds has been proved to be advantageous for methane conversion due to the exothermal feature of the reaction. Hence, other components can be tested for the same reason. Combustion with rich methane also deserves research, as a comparison to lean methane combustion.

5.2.2 Kinetics and temperature profile inside of the reactor

In this project two thermocouples were used to measure the axial temperature in the reactor. As mentioned before, temperature contributes to some key phenomena. For example, the so called “unusual hysteresis” may be due to the strong negative impacts of water, but the measurement of temperature probably has some contributions, too. With a profound temperature profile inside of the reactor, this hypothesis could be justified or excluded.

After the clarification of temperature profile, detailed work about kinetics can be carried out for better understanding of the reaction. Usually the apparent

activation energy will change sharply with the elevation of temperatures. Computer simulation can be employed using different models from Langmuir-Hinshelwood type, to Mars-van Krevelen type, and Eley-Rideal type.

5.2.3 Various pretreatments

In this project three kinds of pretreatments are used: aging in air for all catalyst samples, plus oxidation in air and reduction in hydrogen for selective samples. It has been proved that aging will steady the performance of catalysts, whereas reduction leads to an improvement in activity over original ones. Likewise, some other pretreatments can also bring benefits to catalysts. For instance, Sekizawa et al., (1996) showed that the hysteresis of methane combustion on Pd catalysts was strongly influenced by various of pretreatments at high temperature Lapisardi et al., (2007) tested the catalytic behaviors of Pd catalysts with added Pt and found out that a mild steam aging with 10 % water at 600 ° C could increase the activity of the catalysts by forming an interaction between Pd and Pt particles.

5.2.4 Catalyst characterizations

X-ray diffraction and neutron activation analysis was used here to investigate the composition of catalysts in addition to different Pd phases produced by various treatments. Since major controversies about Pd catalysts raises from phase transformation, it will be an excellent supplement to investigate catalysts via TEM for better realization of the results from aging, reduction and oxidation. Other characterization technologies such as XPS and TGA will give us an overall profile from porosity to reaction mechanism of the catalysts, and information about particle sizes, which is a key parameter for the activity and deactivation of catalysts can be obtained through TEM studies.

Another cause to emphasize catalyst characterization is to comprehend the composition of catalysts as possible justifications for these interesting unusual behaviors such as methane inhibition, which is usually neglected in reported studies. One simple explanation for methane inhibition is water. With the increase of methane concentration, more water is generated, leading to the more severe deactivation of catalysts. However, this can not answer why methane inhibition was always trivial in previous studies where catalysts were also seriously harmed by water. Given that there some additives other that Pd on the catalysts used in this project, detailed investigation on catalyst composition may provide important feedbacks on methane inhibition, catalysts activity, etc.

5.2.5 Pt-Pd bimetallic catalysts

Palladium based catalysts are popular in industry mostly because of their good activity as well as low prices, but their performance is indeed not as stable as platinum based catalysts. Recently may researchers have concentrated on the study of Pd-Pt bimetallic catalysts, believed to combine the advantages of both Pd and Pt catalysts.

Persson et al. (2007) noted that the adding of platinum in palladium based catalysts would stabilize their performance. The conversion of methane oxidation on monometallic palladium catalysts on alumina will gradually decrease with time. When additional water vapor is added into the reaction system, Pd/Al_2O_3 catalysts lose their activity quickly, and this activity can not be fully recovered even after the water is removed. On the other hand, for Pd-Pt bimetallic catalysts, the conversion is much more stable than Pd catalysts. Although Pd-Pt catalyst behavior is also harmed by extra water in the feed, the deactivation is less severe and the lost activity is completely recovered when the water feed is stopped. This is verified by Lapisardi et al.,

(2007), who also suggests that the improvement brought by Pt addition should be attributed to an interaction between Pd and Pt, although Pt addition to Pd did not improve the resistance to sulphur poisoning. Narui et al., (1999) studied the influence of additional Pt on supported catalyst particles by SEM, and discovered that Pt-Pd interaction caused better dispersions of particles on supports and the growth, migration and sintering of catalytic particles was inhibited, which lead to not only a better stability, but also a considerable increase in activity of the catalysts. Based on these discoveries, it will be worthwhile to try new catalysts with both Pd and Pt for low temperature combustion of methane.

5.2.6 Further study on catalyst deactivation and recovery

Decreasing deactivation is crucial for the successful application of this type of catalyst. In this project catalyst samples did not show satisfying resistance to additional water, and their activities could no be fully recovered. Catalyst supports may be responsible for it. Most unrecoverable deactivation of water is observed on HSA γ-alumina (Ribeiro et al., 1994, Datye et al., 2000), whereas on LSA α-alumina water poisoning can be saved (Ciuparu et al.,2002). Other Efforts should be stressed to study treatments to recover activity as fast as possible.

References

Arrosio, F., Colussi, S., Groppi, G., and Trovarelli, A., (2007). Regeneration of S-poisoned Pd/Al_2O_3 and $Pd/CeO_2/Al_2O_3$ catalysts for the combustion of methane. *Topics in Catalysis*, 42-43 (1-4): 405-408.

Baldwin, T. R., and Burch, R., (1990). Catalytic combustion of methane over supported palladium catalysts. II. Support and possible morphological effects. *Applied Catalysis*, 66: 359-381.

Burch, R., and Loader, P. K., (1994). Investigation of Pt/Al_2O_3 and Pd/Al_2O_3 catalysts for the combustion of methane at low concentrations. *Applied Catalysis B: Environmental*, 5 (1-2): 149-164.

Choudhary, V. R., and Rane, V. H., (1992). Pulse microreactor studies on conversion of methane,ethane and ethylene over rare earth oxides in the absence and presence of free oxygen. *Journal of Catalysis*, 135: 310-316.

Choudhary, V. R., Rane, V. H., and Chaudhari, S. T., (1997). Surface property of rare earth promoted MgO catalysts and their activity/selectivity in oxidative coupling of methane. *Applied Catalysis A: General*, 158: 121-136.

Ciuparu, D., Altman E. and Pfefferle, L., (2001). Contributions of lattice oxygen in methanecombustion over PdO-based catalysts. *Journal of Catalysis*, 203 (1): 64-74.

Ciuparu, D., Lyubovsky, M. R., Altman E. Pfefferle, L. D., and Datye, A., (2002). Catalytic combustion of methane over palladium-based catalysts.

Catalysis Review, 44 (4): 593-649.

Cullis, C. F., Nevell, T. G., and Trimm, D. L., (1972). Role of the catalyst support in the oxidation of methane over palladium. *Journal of the Chemical Society, Faraday Transactions 1: Physical Chemistry in Condensed Phases* , 68: 1406-1412.

Cullis, C. F., and Williatt, B. M., (1983). Oxidation of methane over supported precious metal catalysts. *Journal of Catalysis*, 83: 267-285.

Cullity, B. D., (1978). *Elements of X-Ray Diffraction, 2nd Edition.* Addison-Wesley

Datye, A., Bravo, J., Nelson, T. R., Atanasova, P., Lyubovsky, M., and Pfefferle, L., (2000). Catalyst microstructure and methane oxidation reactivity during the Pd↔PdO transformation on alumina supports. *Applied Catalysis A: General*, 198 (1-2): 179-196.

Escandon, L. S., Ordóñez, S., Vega, A., and Díez, F., V., (2005). Oxidation of methane over palladium catalysts: effect of the support. *Chemosphere*, 58: 9-17.

Fino, D., Ruso, N., Saracco, G., and Specchia, V., (2007). Supported Pd-perovskite catalyst for CNG engines' exhaust gas treatment. *Progress in Solid State Chemistry*, 35: 501-511.

Fujimoto, K., Ribeiro, F. H., Avalos-Borja, M., and Iglesia, E., (1998). Structure and reactivity of PdO_x/ZrO_2 catalysts for methane oxidation at low temperatures. *Journal of Catalysis*, 179 (2): 431-442.

Gélin, P., and Primet, M., (2002). Complete oxidation of methane at low temperature over noble metal based catalysts. *Applied Catalysis B: Environmental*, 39: 1-37.

Gélin, P., Urfels, L., Primet, M., and Tena, E., (2003). Complete oxidation of methane at low temperature over Pt and Pd catalysts for the abatement of lean-burn natural gas fuelled vehicles emissions: influence of water and sulphur containing compounds. *Catalysis Today*, 83: 45-57.

Hayes, R., and Kolaczkowski, S., (1997). *Introduction to Catalytic Combustion.* Gordon and Breach Science Publishers.

Hayes, R. E, Kolaczkowski, S. T., Li., P. K. C., and Awdry, S., (2001). The palladium catalysed oxidation of methane: reaction kinetics and the effect of diffusion barriers. *Chemical Engineering Science*, 56: 4815-4835

Hoyos, L. J., Praliaud, H, and Primet, M., (1993). Catalytic combustion of methane over palladium supported on alumina and silica in presence of hydrogen sulfide. *Applied Catalysis A: General*, 98 (2): 125-138.

Hurtado, P., Ordóñez, S., Sastre, H., and Díez, F., V., (2004). Combustion of methane over palladium catalyst in the presence of inorganic compounds: inhibition and deactivation phenomena. *Applied Catalysis B: Environmental*, 47(2): 85-93.

IPCC, "Summary for Policymakers": *Climate Change 2007: The Physical Science Basis. Contribution of Working Group I to the Fourth Assessment Report of the Intergovernmental Panel on Climate Change*. http://ipcc-wg1.ucar.edu/wg1/Report/AR4WG1_Print_SPM.pdf, July 25th, 2009

Kiehl, J. T., and Trenberth K. E, (1997). Earth's Annual Global Mean Energy Budget. *Bulletin of the American Meteorological Society* 78 (2): 197–208

Larpisardi, G., Gélin, P., Kaddouri, A., Garbowski, E., and Da Costa. S, (2007). Pt-Pd bimetallic catalysts for methane emissions abatement. *Topics in Catalysis* 42-43: 461–464

Lee, J. H., and Trimm D. L, (1995). Catalytic combustion of methane. *Fuel Processing Technology* 42 (2-3): 339–359

Litto, R. M., (2008). *Catalytic combustion for mitigation of lean methane emission.* PhD Thesis, University of Alberta

Lyubovsky, M., and Pfefferle, L, (1998). Catalytic combustion of methane. *Applied Catalysis A: General* 173 (1): 107–119

Machoki, A., Rotko, M., and Gac, W., (2009). Steady state isotopic transient kinetic analysis of flameless methane combustion over Pd/Al_2O_3 and Pt/Al_2O_3 catalysts. *Topics in Catalysis*, 52: 1085-1097.

Meeyoo, V., Trimm, D. L., and Cant, N. W., (1998). The effect of sulphur containing pollutants on the oxidation activityof precious metals used in vehicle exhaust catalysts. *Applied Catalysis B: Environmental*, 16: L101-L104.

Müller, C. A., Maciejewski, M., Koeppel, R. A., Tschan, R., and Baker, L., (1996). Role of lattice oxygen in the combustion of methane over PdO/ZrO2: Combined pulse TG-DTA and MS study with ^{18}O-labeled catalyst. *Journal of Physical Chemistry*, 100: 20006-20014.

Narui, K., Yata, H., Furuta, K., Nishida, A., Kohtoku, Y., and Mastuzaki, T., (1999). Effects of addition of Pt to PdO/Al_2O_3 catalyst on catalytic activity for methane combustion and TEM observations of supported Particles. *Applied Catalysis A: General*, 179: 165-173.

Niwa, M., Awano K., and Murakami, Y., (1983). Activity of supported platinum catalysts for methane oxidation. *Applied Catalysis*, 7 (3): 317-325.

Ozawa, Y., Tochihara, Y., Nagai, M., and Omi, S., (2003). PdO/Al_2O_3 in catalytic combustion of methane: stabilization and deactivation. *Chemical Engineering Science*, 58: 671-677.

Ozkan, U. S., Kumthekar, M. W., and Karakas, G., (1997). Self-sustained oscillatory behavior of $NO+CH_4+O_2$ reaction over titania-supported Pd catalysts. *Journal of Catalysis*, 171 (1): 67-76.

Persson, K., Pfefferle, L. D, Schwartz, W., Ersson, A., and Järås, S. D., (2007). Stability of palladium-based catalysts during catalytic combustion of methane-The influence of water. *Applied Catalysis B: Environmental*, 74: 242-250.

Ribeiro F. H., Chow M. and Dallabetta R. A., (1994). Kinetics of the complete oxidation of methane over supported palladium catalysts. *Journal of Catalysis*, 146 (2): 537-544.

Roth, D., Gélin, P., Kaddouri, A., Garbowski, E., Primet, M., and Tena, E., (2006). Oxidation behaviour and catalytic properties of Pd/Al2O3 catalysts in the total oxidation of methane. *Catalysis Today*, 112: 134-138.

Salaün, M., Kouakou, A., Da Costa, S., and Da Costa, P., (2009). Synthetic gas bench study of a natural gas vehicle commercial catalyst in monolithic form: On the effect of gas composition. *Applied Catalysis B: Environmental*, 88: 386-397.

Salomons, S., Hayes, R. E., Poirier, M., and Sapoundajiev, H., (2003). Flow reversal reactor for the catalytic combustion of lean methane mixtures. *Catalysis Today*, 83: 59-69.

Sekizawa K., Eguchi, K., Poirier, M., Widjaja, H., Machida, M., and Arai, H., (1996). Property of Pd-supported catalysts for catalytic combustion. *Catalysis Today*, 28 (3): 245-250.

Schmal, M., Souza, M. M. V. M., Alegre, V. V., da Silva M. V. P., César, D. V., and Perez, C. A. C., (2006). Methane oxidation - effect of support, precursor and pretreatment conditions - in situ reaction XPS and DRIFT. *Catalysis Today*, 118: 392-401.

van Giezen, J. C., van den Berg, F. R., Kleinen, J. L., van Dillen A. J., and Geus**,** J. W., (1999). The effect of water on the activity of supported palladium catalysts in the catalytic combustion of methane. *Catalysis Today*, 47 (1-4): 287-293.

Voltz, S. E., Morgan, C. R., Liederman, D., and Jacob, S. M., (1973). Kinetic study of carbon monoxide and propylene oxidation on platinum catalysts. *Industrial & Engineering Chemistry Product Research and Development,* 12 (4): 294-301

Appendix A List of runs

List of runs for methane oxidation[a]								
Run #	**Catalyst, g/ft^3**	**Procedure[b]**	**Reduction**	**Oxidation**	**CH_4, mL/min**	**CH_4, ppm**	**T, °C**	**Water, 5% mol**
401-425	150	exploratory runs			9.75	4700± 150	-	N
426	150	I	15 min	N	9.75	4700± 150	300~ 450	N
427	150	I-E	-	-	9.75	4700± 150	450~ 300	N
428	150	I	15 min	N	9.75	4700± 150	300~ 450	N
429	150	I-E	-	-	9.75	4700± 150	450~ 300	N
430	150	I	15 min	N	9.75	4700± 150	300~ 450	N
431	150	I-E	-	-	9.75	4700± 150	450~ 300	N
432	150	E	15 min	520°C, 2.5 h	9.75	4700± 150	500~ 300	N
433	150	E	15 min	520°C, 2.5 h	9.75	4700± 150	500~ 300	N
434	150	E	15 min	450°C, 2.5 h	9.75	4700± 150	500~ 300	N
435	150	E	15 min	450°C,1 h	9.75	4700± 150	500~ 300	N
436	150	E	15 min	450°C, 15 min	9.75	4700± 150	500~ 300	N
437	150	E	15 min	520°C, 5 h	9.75	4700± 150	500~ 300	N
438	150	E	N2/870°C/ 2.5h	N	9.75	4700± 150	500~ 300	N

Run #	Catalyst, g/ft^3	Procedure[b]	Reduction	Oxidation	CH_4, mL/min	CH_4, ppm	T, °C	Water, 5% mol
439	150	E	N2/870°C/ 2.5h	N	9.75	4700± 150	850~ 300	N
440	150	E	N2/870°C/ 2.5h	N	9.75	4700± 150	850~ 300	N
501	80	I	15 min	N	9.75	4700± 150	300~ 450	N
502	80	I-E	-	-	9.75	4700± 150	450~ 300	N
503	80	E	15 min	N	9.75	4700± 150	500~ 300	N
504	80	E	15 min	N	9.75	4700± 150	500~ 300	N
505	80	I	15 min	N	9.75	4700± 150	200~ 400	N
506	80	I-E	-	-	9.75	4700± 150	400~ 200	N
507	80	I	N	N	9.75	4700± 150	200~ 450	N
508	80	I-E	-	-	9.75	4700± 150	450~ 200	N
509	80	E	15 min	N	9.75	4700± 150	400~ 250	N
510	80	E	15 min	520°C, 5 h	9.75	4700± 150	450~ 250	N
511	80	E	15 min	520°C, 1 h	9.75	4700± 150	400~ 200	N
601	15	I	15 min	N	9.75	4700± 150	300~ 600	N
602	15	I-E	-	-	9.75	4700± 150	600~ 300	N
603	15	I	15 min	N	9.75	4700± 150	300~ 600	N
604	15	I-E	-	-	9.75	4700± 150	600~ 300	N
605	15	I	15 min	N	9.75	4700± 150	300~ 600	N
606	15	I-E	-	-	9.75	4700± 150	600~ 300	N

Run #	Catalyst, g/ft^3	Procedure[b]	Reduction	Oxidation	CH_4, mL/min	CH_4, ppm	T, °C	Water, 5% mol
607	15	E	15 min	N	9.75	4700±150	600~300	N
608	15	I	15 min	N	19.75	8500±300	300~600	N
609	15	I-E	-	-	19.75	8500±300	600~300	N
610	15	I	15 min	N	6.00	3100±100	300~600	N
611	15	I-E	-	-	6.00	3100±100	600~300	N
612	15	E (D)	15 min	N	9.75	4700±150	600-480(2h)300 N	
613	15	E	15 min	520°C, 5 h	9.75	4700±150	600~300	N
614	15	E	15 min	520°C, 5 h	19.75	8500±300	600~300	N
615	15	E	15 min	520°C, 5 h	6.00	3100±100	600~300	N
616	15	E	15 min	520°C, 1 h	9.75	4700±150	400~200	N
617	15	E	15 min	520°C, 2 h	9.75	4700±150	400~200	N
701	150	I	Y, 15 min	N	9.75	4700±150	200~350	N
702	150	I-E	-	-	9.75	4700±150	350~200	N
703	150	E	15 min	N	9.75	4700±150	400~200	N
704	150	E	15 min	520°C, 5 h	9.75	4700±150	400~200	N
705	150	I	15 min	N	19.75	8500±300	200~200	N
706	150	I-E	-	-	19.75	8500±300	400~200	N
707	150	E	15 min	N	19.75	8500±300	400~200	N
708	150	E	15 min	N	19.75	8500±300	400~200	N

Run #	Catalyst, g/ft^3	Procedure[b]	Reduction	Oxidation	CH_4, mL/min	CH_4, ppm	T, °C	Water, 5% mol
709	150	I	15 min	N	6.00	3100± 100	200~ 300	N
710	150	I-E	-	-	6.00	3100± 100	300~ 200	N
711	150	E	15 min	N	6.00	3100± 100	400~ 200	N
712	150	E	15 min	520°C, 5 h	6.00	3100± 100	400~ 200	N
801	150	I	15 min	N	9.75	4700± 150	200~ 350	Y
802	150	I-E	-	-	9.75	4700± 150	350~ 200	Y
803	150	I	15 min	N	9.75	4700± 150	200~ 550	Y
804	150	I-E	-	-	9.75	4700± 150	550~ 200	Y
805	150	I	45 min	N	9.75	4700± 150	200~ 550	Y
806	150	I-E	-	-	9.75	4700± 150	550~ 200	Y
807	150	E	135 min	N	9.75	4700± 150	400~ 200	Y
808[c]	150	I	75 min	520°C, 5 h	9.75	4700± 150	200~ 550	Y
809	150	I-E	-	-	9.75	4700± 150	550~ 200	Y
810	150	I	75 min	N	9.75	4700± 150	200~ 550	Y
811	150	I-E	-	-	9.75	4700± 150	550~ 200	Y
901	150	I	15 min	N	9.75	4700± 150	200~ 400	Y
902	150	I-E	-	-	9.75	4700± 150	400~ 300	Y
903	150	I	15 min	N	9.75	4700± 150	200~ 400	Y

Run #	Catalyst, g/ft^3	Procedure[b]	Reduction	Oxidation	CH_4, mL/min	CH_4, ppm	T, °C	Water, 5% mol
904	150	I-E	-	-	9.75	4700± 150	400~ 300	Y
905	150	I	15 min	N	9.75	4700± 150	200~ 500	Y
906	150	I-E	-	-	9.75	4700± 150	500~ 300	Y
907[c]	150	I	15 min	520°C, 5 h	9.75	4700± 150	200~ 600	Y
908	150	I-E	-	-	9.75	4700± 150	600~ 300	Y
909	150	I	15 min	N	9.75	4700± 150	200~ 600	Y
910	150	I-E	-	-	9.75	4700± 150	600~ 300	Y
911	150	I	15 min	N	9.75	4700± 150	200~ 500	Y
912	150	I-E	-	-	9.75	4700± 150	500~ 300	Y
913	150	I	N	N	9.75	4700± 150	200~ 600	Y
914	150	I-E	-	-	9.75	4700± 150	600~ 400	Y
915	150	I	N	N	9.75	4700± 150	200~ 650	Y
916	150	I-E	-	-	9.75	4700± 150	650~ 400	Y
917	150	I	N	N	9.75	4700± 150	200~ 650	Y
918	150	D	N	N	9.75	4700± 150	585, 17 h	Y
919	150	D	N	N	9.75	4700± 150	585, 25 h	Y
920	150	-	-	-	-	-	-	-
921	150	I	N	N	9.75	4700± 150	200~ 600	N
922	150	I-E	-	-	9.75	4700± 150	600~ 360	N
923	150	I	N	N	9.75	4700± 150	200~ 600	N

Run #	Catalyst, g/ft^3	Procedure[b]	Reduction	Oxidation	CH_4, mL/min	CH_4, ppm	T, °C	Water, 5% mol
924	150	I-E	-	-	9.75	4700± 150	600~ 350	N
925	150	I	N	N	9.75	4700± 150	200~ 650	N
926	150	I-E	-	-	9.75	4700± 150	650~ 350	N
927	150	I	15 min	N	9.75	4700± 150	200~ 550	N
928	150	I-E	-	-	9.75	4700± 150	550~ 300	N
929	150	I	15 min	N	9.75	4700± 150	200~ 550	N
930	150	I-E	-	-	9.75	4700± 150	550~ 300	N
931	150	D	N	N	9.75	4700± 150	585, 29 h	stop at 24 h
932	150	D	N	N	9.75	4700± 150	585, 60 h	stop at 51 h
933	150	after 932, D	N	N	9.75	4700± 150	585, 5 h	N
Note:								
[a]. The flow rate of air was fixed at 198.00 mL/min. The mass of catalyst samples for all the runs								
was 1.20 g, except for Run# 04XX, some catalysts were lost.								
[b]. I=ignition, E=extinction, I-E=extinction after ignition, D=deactivation								
[c]. Oxidation was done before reduction.								